

2

AD-A247 455



DTIC
ELECTE
MAR 10 1992
S C D

Document 381-92



METEOROLOGICAL MEASUREMENTS GUIDE

METEOROLOGY GROUP

RANGE COMMANDERS COUNCIL

- WHITE SANDS MISSILE RANGE
- KWAJALEIN MISSILE RANGE
- YUMA PROVING GROUND
- ELECTRONIC PROVING GROUND
- DUGWAY PROVING GROUND

- NAVAL AIR WARFARE CENTER-WEAPONS DIVISION, PT MUGU
- NAVAL AIR WARFARE CENTER-WEAPONS DIVISION, CHINA LAKE
- ATLANTIC FLEET WEAPONS TRAINING FACILITY
- NAVAL AIR WARFARE CENTER-AIRCRAFT DIVISION, PATUXENT RIVER
- NAVAL UNDERWATER SYSTEMS CENTER

- 45TH SPACE WING
- AIR FORCE DEVELOPMENT TEST CENTER
- 30TH SPACE WING
- CONSOLIDATED SPACE TEST CENTER
- AIR FORCE FLIGHT TEST CENTER
- AIR FORCE TACTICAL FIGHTER WEAPONS CENTER

*DISTRIBUTION STATEMENT A: APPROVED FOR PUBLIC RELEASE;
DISTRIBUTION UNLIMITED.*

92-06039



92 3 06 023

January 1992

METEOROLOGICAL MEASUREMENTS GUIDE

Meteorology Group
Range Commanders Council
White Sands Missile Range, NM 88002-5110

RCC Document 381-92

Range Commanders Council
STEWS-SA-R
White Sands Missile Range, NM 88002-5110

same as block 8

New document

APPROVED FOR PUBLIC RELEASE; DISTRIBUTION UNLIMITED

Provides guidance to users of meteorological instrumentation who are tasked with producing reliable measurements; that is, instruments functioning with required precision and accuracy, and measurements representative of the phenomenon to be measured. It is designed to serve as a general guide to the use of meteorological instruments.

meteorological measurements, remote sensing instruments,
passive remote sensing, airborne instruments, active remote
sensing

90

UNCLASSIFIED

UNCLASSIFIED

UNCLASSIFIED

NONE

DOCUMENT 381-92

METEOROLOGICAL MEASUREMENTS GUIDE

JANUARY 1992



Accession For	
DTIC GRA&I	<input checked="" type="checkbox"/>
DTIC Tab	<input type="checkbox"/>
Unannounced	<input type="checkbox"/>
Justification	
By	
Distribution/	
Availability Codes	
Dist	Avail and/or Special
A-1	

Prepared by

Meteorology Group
Range Commanders Council

Published by

Secretariat
Range Commanders Council
U.S. Army White Sands Missile Range,
New Mexico 88002

FOREWORD

This document was prepared by the Range Commanders Council (RCC), Meteorology Group (MG) to satisfy the requirements of task MG-6, Establish Guidelines for Calibration Intervals and Procedures for Non-Standard Meteorological Instrumentation. This task was undertaken by the Standing Committee on Meteorological Measurements, Christopher A. Bilstoft, Chairperson, with collaboration by Richard Hasbrouck (Standing Committee on Lightning Prediction and Detection) and Robert Smith (Standing Committee on Electro-Optics). Document review and comment were provided by the following MG members:

E. Hatfield
H. Herring
P. Harvey
J. Kerwin
N. Harris
L. Corbett

D. Weingarten
D. Tolzin
L. Hall
L. Corbett
G. Boire
F. Hauth

J. Sniscak
R. Olsen
G. Phelps
F. Schmidlin
R. Kren

TABLE OF CONTENTS

	<u>Page</u>
Foreword.....	iii
CHAPTER 1 - INTRODUCTION.....	1-1
CHAPTER 2 - FIXED-POINT INSTRUMENTS	
Anemometers.....	2-1
Cup Anemometers.....	2-1
Propeller Anemometers.....	2-5
Sonic Anemometers/Thermometers.....	2-6
Thermal Anemometry.....	2-8
Other Nonmechanical Anemometers.....	2-9
Wind Vanes.....	2-9
Thermometers and Radiation Shields.....	2-11
Platinum Wire Platinum-Resistance Thermometers.....	2-12
Thermoelectric Thermometers (Thermocouples).....	2-12
Thermistors.....	2-13
Quartz-Crystal Thermometers.....	2-14
Liquid-in-Glass Thermometers.....	2-17
Hygrometers.....	2-17
Lithium-Chloride Dew Cell.....	2-18
Chilled-Mirror Hygrometers.....	2-19
Adsorption Hygrometers.....	2-20
Lyman- α Hygrometers.....	2-20
Infrared Hygrometers.....	2-21
Psychrometers.....	2-21
Hair Hygrothermograph.....	2-22
Barometers.....	2-22
Mercury Barometers.....	2-23
Aneroid Barometers.....	2-23
Digital Barometers.....	2-23
Precipitation Sensors.....	2-23
Mechanical Gages.....	2-24
Optical-Precipitation Sensors.....	2-24
CHAPTER 3 - ACTIVE REMOTE-SENSING INSTRUMENTS	
Doppler-Acoustic Sounders.....	3-2
Radar-Wind Profilers.....	3-5
Scintillometers.....	3-8
Finite-Aperture Scintillometers.....	3-10
Spatially-Averaged Filter Scintillometers.....	3-11
Other Remote Sensors and Remote Sensor Combinations.....	3-13
Visibility Meters.....	3-14
Transmissometers.....	3-14

CHAPTER 4 - PASSIVE REMOTE-SENSING INSTRUMENTS

Radioactive Probes.....	4-1
Corona-Current Systems.....	4-3
Electric-Field Mills.....	4-3
Pre-Cloud-to-Ground Lightning Warning and Cloud-to-Ground Lightning Tracking.....	4-5
Sferics Detectors.....	4-5
Electro-Optical Sensors.....	4-5
Locating Intracloud Discharges.....	4-6
Magnetic-Direction Finding.....	4-6
Time-of-Arrival.....	4-6
Radiometric Profilers.....	4-7
Plant-Canopy Analyzer.....	4-7
Actinometers.....	4-8
Pyranometers.....	4-8
Pyrgeometers.....	4-9
Pyrheliometers.....	4-10

CHAPTER 5 - AIRBORNE INSTRUMENTS

Free Balloons.....	5-1
Pilot Balloons.....	5-3
Jimspheres.....	5-2
Radiosondes.....	5-3
Loran Systems.....	5-3
Omega Systems.....	5-4
Radio Direction-Finding Systems.....	5-4
Tethered Balloons and Kites.....	5-4
Rocketsondes and Mini-Rocketsondes.....	5-5
Dropsondes.....	5-5
Aircraft-Sensor Platforms.....	5-6

CHAPTER 6 - SAMPLING AND QUALITY CONTROL

Sampling and Averaging Time.....	6-1
Site Influences.....	6-3
Quality Control.....	6-4
Wind-Data Processing.....	6-6
Intercomparison Testing.....	6-7
Transfer-Standard Method.....	6-8
Variance-Estimates Method.....	6-8

GLOSSARY OF TERMS**REFERENCES**

LIST OF FIGURES

	<u>Page</u>
2-1 Fluctuating signal components from a fast response micrometeorological cup anemometer (solid line) and a sonic anemometer (dashed line) in response to a turbulent wind field (Biltoft, 1989).....	2-4
2-2 Near instantaneous response of a sonic thermometer (upper curve) and the slower response of fiber-optic quartz thermometer (lower curve).....	2-15
3-1 Hourly consensus data from the Dugway Proving Ground radar wind profiler (Source: Wang et al., (1991)).....	3-9
3-2 Theoretical weighting functions for the (a) WPL Models II and IV finite aperture scintillometers, and (b) the spatially-averaged filter scintillometer.....	3-12
4-1 Typical evolution of the surface potential gradient during a thunderstorm event. The typical fair-weather field gradient is 100-200 V/m (A). As the storm develops a field polarity reversal occurs (B) and magnitude of the potential gradient increases, exceeding the "warning" and "danger" levels. Lightning-induced spikes occur (C) as based sensors. The declining phase (E) is characterized by few (if any) lightning events, and the potential gradient again crosses zero (F) and reverts to a fair-weather polarity and intensity (G). (Source: Airborne Research Associates, Inc.).....	4-2

LIST OF TABLES

2-1 RECOMMENDED RESPONSE CHARACTERISTICS FOR CUP AND PROPELLER ANEMOMETERS, HORIZONTAL WIND VANES, AND BIVANES.....	2-6
3-1 TYPES OF WIND-PROFILING RADARS.....	3-7
4-1 TYPICAL ACTINOMETER RESPONSE.....	4-10
6-1 REASONABLENESS AND CONSISTENCY CRITERIA FOR METEOROLOGICAL DATA.....	6-5

CHAPTER 1

INTRODUCTION

This document provides guidance to users of meteorological instrumentation who are tasked with producing reliable measurements; that is, instruments functioning with required precision and accuracy, and measurements representative of the phenomenon to be measured. It is designed to serve as a general guide to the use of meteorological instruments available at Range Commanders Council, Meteorology Group (RCC-MG) member ranges. Accordingly, each instrument subsection includes (1) a description of the instrument and how it operates, (2) a discussion of the instrument's capabilities and limitations, (3) estimates of resolution and accuracy, and (4) guidance on calibration and quality control procedures. References are provided for detailed technical and procedural information.

Additionally, this document is organized into general categories of instruments: those that make measurements at fixed points in space, active remote sensing instruments, passive remote sensing instruments, and airborne instruments. Appendixes on sampling and quality control and a glossary of terms follow. Fixed-point instruments are placed at a specific location to obtain measurements at that location. Active remote sensors rely on the reception of forward- or backscattered energy as a means of obtaining information from the atmosphere. Passive remote sensors obtain information without requiring a transmitter as part of the instrumentation. Airborne instruments are unique by virtue of a platform, including aircraft and various types of balloons and kites that carry the sensors through the air.

CHAPTER 2

FIXED-POINT INSTRUMENTS

Fixed-point instruments such as anemometers, wind vanes, and thermometers are the most common and usually the least expensive meteorological sensors. They are often mounted on meteorological towers or in instrument shelters. Fixed-point sensors offer the advantages of well understood operating characteristics and simplicity. Instrument output is often related to the measured variable through a transfer function defined in a laboratory. Also, many of these instruments have simple calibration procedures. In turn, a fixed-point instrument is limited to sampling portions of the atmosphere flowing past its sensor. Because of their physical presence, fixed point sensors and their supporting structures perturb the atmosphere in which they are immersed. Additionally, measurements made at a fixed point can be unrepresentative of meteorological conditions occurring at locations where measurements are needed. Representativeness can be particularly true of measurements taken close to the Earth's surface for atmospheric dispersion applications. Detailed theory and a discussion of many types of fixed-point instruments are provided in the *Instructor's Handbook on Meteorological Instrumentation* (Brock and Nicolaidis, 1984).

Anemometers

In-situ instruments used for wind-speed measurements include cup and propeller anemometers; ion beam, thin-film, and hot-wire anemometers; and sonic anemometer/thermometers. Alternative wind measurement instrumentation also exists for specialized applications. Field inter-comparisons of in-situ wind sensors (Finkelstein et al., 1986) indicate that wind-speed measurement biases on the order of 0.15 meters per second (m/s) and comparabilities near 0.35 m/s are possible with high quality cup and propeller anemometers. An analysis of the same data by Lockhart (1989) suggests that agreement to about 0.2 m/s is possible.

Cup Anemometers. A cup anemometer consists of a conical 3-cup (occasionally 6-cup) rotor assembly mounted on a rotating shaft that rests on low friction bearings within a transmitter housing. Wind flowing past the rotor assembly creates an asymmetrical drag because drag coefficients are larger on each cup's concave side than on the convex side. This asymmetrical drag causes an imbalance of forces on the cup surfaces that generates torque on the rotor. The assembly rotates when torque overcomes bearing friction; the speed at which this occurs is the starting threshold. Above threshold speed, a rotor assembly responds to

ambient winds by increasing or decreasing rotation rate to balance forces on the cup surfaces. A light beam chopper within the rotor assembly produces pulse counts proportional to rotation speed. Magnetic or generator-based mechanisms are also available. System response is modulated for high frequency noise by a low-pass filter in the transmitter, and pulse counts are converted to analog voltages by a translator. Transmitter output is related to wind-speed by a transfer function defined in wind tunnel tests. Cup anemometer response has been modeled by Snow et al. (1989).

Cup anemometers offer the advantages of simplicity, ruggedness, and maturity of design, and their operational characteristics have been optimized through extensive testing. The latest designs include strong, lightweight plastics or carbon-fiber composites that achieve structural strength and rigidity with lightweight assemblies. A major advantage offered by cup anemometers is that they are omni-directional in the horizontal plane, requiring no orientation into the wind.

Disadvantages of cup anemometers include inertial effects because of asymmetrical cup drag, non-uniform torque generation, and irregular off-axis response. Inertial effects cause the rotor assembly to gain energy in an accelerating wind field more quickly than it loses energy in a decelerating wind field. Torque generated by aerodynamic drag on cup anemometers is non-uniform, varying with the position of the cup assembly in the flow (Lockhart, 1985). These torque variations cause the rotating cup assembly to be in a continual state of acceleration/deceleration, which produces undesirable high frequency noise signal. The electrical filters used in the transmitter represent an engineering compromise between system response and the need to dampen this noise. The result is a smoothed output with phase lag. These effects are illustrated in figure 2-1, which compares the response of a cup anemometer with the inertia-free response of a sonic anemometer. Cup anemometers also exhibit an irregular off-axis response to vertical wind components (MacCready, 1966). The cumulative effect of these cup anemometer response characteristics is overspeeding, which can reach 3 to 10 percent in turbulent wind conditions (Hayashi, 1987; Kaganov and Yaglom, 1976).

Cup anemometer sensor performance is determined through wind tunnel tests. Performance characteristics include starting threshold, distance constant, and off-axis response (see glossary for definition of terms). These performance characteristics and the sensor transfer function can be defined using American Society for Testing and Materials (ASTM) Method D5096 (1990). Cup anemometer measurement accuracy in a steady horizontal wind can be defined by a transfer function to within 1 or 2 percent of reference speed over the speed range defined by the ASTM method. Outside this range, low-speed frictional drag and high-speed

aerodynamic drag degrade measurement accuracy. The density dependent starting threshold and distance constant will vary from one location to another, but the transfer function and off-axis response remain invariant over the normal range of atmospheric densities. The cup anemometer characteristics recommended by Strimaitis et al. (1981) for dispersion model applications are presented in table 2-1.

Cup anemometer performance is degraded when the cups are deformed, damaged, or when moisture or particles accumulate on them. Cup assemblies in field use should be frequently inspected for damage and accumulation of foreign matter. Anemometer performance also deteriorates as bearing friction increases because of wear. Increased bearing friction is often gradual and difficult to detect in the field unless speeds near starting threshold are closely monitored. Starting threshold or torque checks are recommended every 6 months, supplemented by field intercomparison and wind profile checks (see Quality Control, chapter 6). Damage and the accumulation of foreign matter can be detected through visual inspection of the rotor. Wind tunnel calibration verifies performance of the entire anemometer assembly. Starting torque can be verified using a Waters torque watch or a Young torque disk. These techniques are described in the Quality Assurance Handbook (1989).

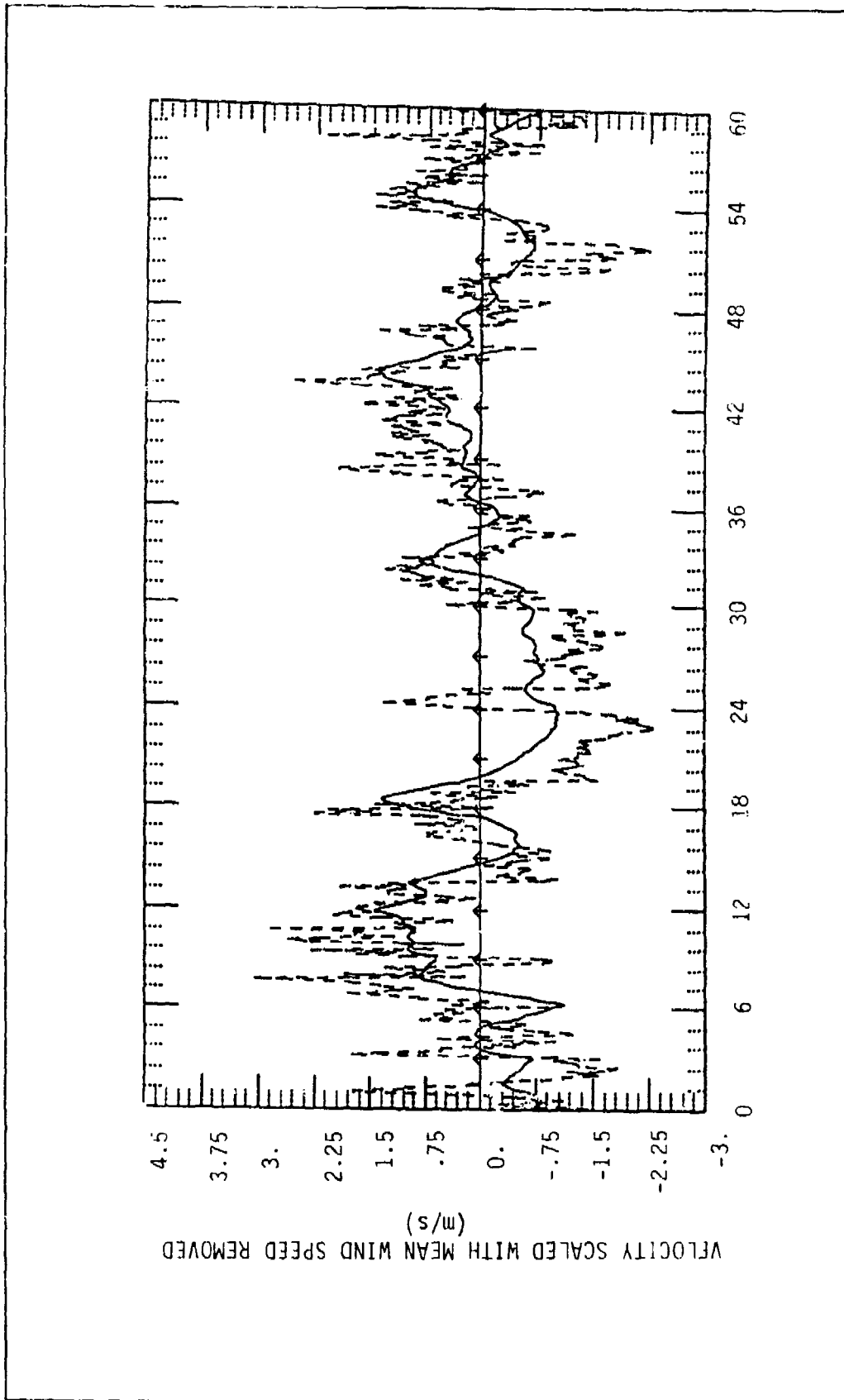


Figure 2-1. Fluctuating signal components from a fast response micrometeorological cup anemometer (solid line) and a sonic anemometer (dashed line) in response to a turbulent wind field (Biltoft, 1989).

Propeller Anemometers. Propeller anemometers consist of a 3- or 4-blade helicoid propeller assembly mounted on a shaft extending into a transmitter housing. The shaft is usually oriented to intercept the horizontal wind flow and can be mounted on the front of a vane for orientation into the wind. Wind blowing past the array generates a torque on the rotor, and the assembly rotates when sufficient torque is generated to overcome bearing friction. The rotor assembly responds to ambient winds by increasing or decreasing rotation until forces on the rotor are in balance. A light chopper generates a pulse count proportional to assembly rotation rate; the count is converted to velocity using a transfer function defined in wind tunnel tests. A similar procedure is used for magnetic and generator-based sensor assemblies. Propeller anemometers can be found in fixed orthogonal (u, v, w) arrays or mounted on the front of vanes.

Propeller anemometers offer the advantages of lightweight, low-starting threshold, and a simple, linear transfer function that remains constant over a wide range of velocities and atmospheric densities (Gill, 1963). These attributes are present because, unlike a cup assembly, the helicoid propeller's surface area is symmetrical about the array axis of rotation and the entire frontal surface area is continuously available for torque generation. Above threshold velocities, propeller anemometer measurement accuracy in a steady on-axis wind can usually be defined within 1 or 2 percent of a reference velocity over a velocity range defined by the ASTM Method D5096 (1990).

The main disadvantages of propeller anemometers derive from their lack of omnidirectional response to the wind. Propellers that are constrained to a fixed position or plane can only respond to the on-axis wind component. To a first order, propeller response is the true wind-speed multiplied by the cosine of the angle of attack. Real propeller arrays also have a small but significant non-cosine component to their off-axis response. In addition, propellers cannot respond properly to the wind when the sensor is near its stall angle (approaching 90° to the wind). Consequently, propeller arrays are often mounted on vanes to keep them oriented into the wind. Failure to correct for non-cosine-response errors can lead to gross errors if the data are used for momentum flux or turbulence measurements. Massman and Zeller (1988) provide a methodology for non-cosine error correction. Overspeeding has also been observed in heavier propeller arrays (Mori and Mitsuta, 1987), although this effect is below detection threshold for modern lightweight arrays.

Pertinent propeller anemometer performance characteristics are starting threshold, distance constant, and off-axis response. Transmitter output is related to velocity by a transfer function. The performance characteristics and transfer function are defined by wind tunnel tests using ASTM Method D5096 (1990). For modern, lightweight helicoid propellers, the performance characteristics

and transfer function remain essentially constant over a normal range of atmospheric densities. Biannual starting threshold or torque checks are recommended to verify calibration. Wind tunnels can verify performance of the sensor assembly at threshold and over the instrument's operating range. Starting torque can be checked using a Waters torque watch or a Young torque disk (Quality Assurance Handbook, 1989). The propeller anemometer characteristics recommended for dispersion model applications are presented in table 2-1. Standard wind and gust measurement procedures are described in the World Meteorological Organization (WMO) Guide (1983).

TABLE 2-1. RECOMMENDED RESPONSE CHARACTERISTICS FOR CUP AND PROPELLER ANEMOMETERS, HORIZONTAL WIND VANES, AND BIVANES

Technical Specification	Cup Anemometer	Propeller Anemometer	Horizontal Vane	Bi-Vane
Accuracy/Precision	±0.2 m/s	±0.2 m/s	+5°	+3°
Resolution	0.1 m/s	0.1 m/s	1°	1°
Threshold	<0.5 m/s	<0.5 m/s	<0.5 m/s	<0.5 m/s
Range	0-50 m/s	0-30 m/s	0-540° (elect.) 0-360° (mech)	+60° (vert)
Distance Constant	<5 m	<5 m	<5 m	<3 m
Damping Ratio	- -	- -	0.4-0.6	0.4-0.6

(Source: Strimaitis et al. (1981)).

Sonic Anemometers/Thermometers. The sonic anemometer/thermometer (sonic) is capable of simultaneously providing wind velocity component and sonic temperature measurements at high data rates. Sonics consist of pairs of transmitters and receivers, spaced 10 to 25 cm apart, that send or receive sound pulses at the rate of several hundred times per second. The fundamental unit of measure for these instruments is time. These instruments operate on the principle that the time between transmission and reception of a sound pulse is a function of the speed of sound

plus the wind-speed component along the transmitter-receiver axis. A time differential is found by subtracting the time taken for travel in one direction from time of travel in the other direction. Because the speed of sound does not change appreciably in the fraction of a second between each transmission, the time differential is assumed to be a component of wind along the transmitter-receiver axis. The horizontal wind vector can be resolved by a sonic with two axes and the three-dimensional wind vector can be resolved by one with three axes. By summing rather than differencing pairs of inverse transit times, the sonic simultaneously provides speed of sound measurements that can be converted to sonic temperatures (Kaimal and Gaynor, 1991).

Unlike mechanical wind sensors, the sonic does not gain or shed energy with the environment for measurement purposes. Therefore, sonics can produce wind component and temperature measurements at fast data rates without inertia, damping, overshoot, or threshold complications. Instrument response is bounded by the rate of acoustic wavefront propagation between transducers (several hundred microseconds) and the instrument's data averaging algorithms. However, the advantages offered by sonic anemometry do not come without penalty. Sonic electronics are fairly complex, and the services of a skilled technician are required to successfully operate and maintain the equipment. Absolute calibration is possible with the use of a zero wind tube in a controlled atmosphere (see ASTM-XXX3). The major remaining difficulties are flow distortion and flow separation because of the physical presence of a sonic array around the sampling volume, although streamlined transducer designs and software corrections have minimized these problems. Sealed transducers permit operation in a wet environment where the performance of mechanical and thermal sensors is degraded. Precise array axis orientation is required for sonic anemometers to eliminate cross-axis signal contamination, and valid wind data can be collected only when flow is within the instruments acceptance angle. Also, substantial software is needed to convert measurements made along a fixed axis of orientation to along wind and crosswind components or to wind-speed and direction. Procedures recommended for sonic operation are described in ASTM-XXX2.

Sonics are typically operated at a data rate of 10 cycles per second (Hz) or greater and are recommended when high quality wind, flux, and turbulence measurements are needed. Sonics provide the wind component and temperature data required for covariance computations. These covariances are then used to compute the fluxes of heat, momentum, and moisture which define the state of the surface boundary layer by the eddy correlation method. These fluxes characterize the atmosphere's stability and dispersion power for diffusion model applications.

Sonic performance is defined in terms of the standard error of the velocity estimate, thermal stability, velocity range, and acceptance (see ASTM-XXX3). Acoustic pathlength and transducer shadow corrections are also needed to characterize a sonic anemometer/thermometer. A sonic's turbulence measurement capability is limited by its spatial resolution. Spatial resolution is defined by the acoustic pathlength and angle of orientation into the flow (Silverman, 1968). Calibration is verified by checking the acoustic pathlength with calipers and performing the zero wind chamber calibration procedure specified in ASTM-XXX3. Sonic anemometer performance is discussed in Kaimal et al. (1990). Kraan and Oost (1989) describe calibration procedures for sonics with nonorthogonal axes.

Thermal Anemometry. This class of nonmechanical anemometers is based on King's law, which relates heat dissipation in a wire to the square root of velocity normal to the wire. A similar relationship applies to hot film sensors. Thermal anemometers contain a set of hot-wire or hot-film sensors mounted in an electrical bridge network. In a zero-wind field, the bridge network is in balance with the hot element maintained at a specified temperature. The cooling effect of the wind blowing across the long axis of the sensor generates a bridge current and produces an analog voltage output. The horizontal wind vector can be resolved by a set of orthogonally mounted hot-wire sensor elements.

Hot-wire or hot-film anemometers offer the advantages of small size, rapid response (data rates of several hundred Hertz are possible), and the ability to measure flow in a confined area. Disadvantages include sensitivity to contamination, which can change sensor calibration, and fragility. Covers or shields are sometimes used to protect sensors. These instruments also need air density compensation. Density compensation is required because heat dissipation is a molecular process and a density correction accounts for sensor contact with a varying number of molecules per unit volume at different elevations with respect to sea level. An additional problem with hot-wire and hot-film anemometers is that inherent nonlinearities, flow blockage, and distortion effects generated by a protective cover make wind-tunnel calibration a complex process. The covers or shields distort off-axis response; sensor orientation can be a major operational consideration.

Significant progress has recently been made in the design of rugged hot-wire and hot-film anemometers that are relatively insensitive to contamination, although their usefulness remains questionable in wet conditions. New micro-processors that accommodate high-order calibration equations and density compensation routines make these instruments accurate nonmechanical

flow measurement devices. Hot-wire or hot-film anemometers are the instruments of choice when high frequency turbulence measurements are needed within 1 m of the surface or in confined areas. However, hot wire anemometers respond to temperature fluctuations as well as velocity, creating significant uncertainty in velocity-temperature correlation data. The effects of hot-wire dynamic response are discussed by Larsen et al. (1986). Fine scale velocity and temperature measurement applications are summarized in Lenschow (1986).

Thermal anemometer calibration involves determination of sensor temperature-resistance characteristics, angular (yaw) response, and heat transfer in forced convection (Andreas and Murphy, 1986). Calibration points are taken in zero wind and at several wind-speeds. Andreas and Murphy conclude that the temperature coefficient of resistance is sufficiently stable for platinum hot-film anemometers that full annual recalibration is probably unnecessary if the reference resistance remains stable.

Other Nonmechanical Anemometers. Additional nonmechanical anemometers are based on technologies such as ion-beam deflection and wake-vortex generation. While they hold promise, these technologies are not as well developed as other wind measurement technologies. Advantages of these instruments include less sensitivity to contamination than hot-wire anemometers and increased ruggedness. Universally accepted calibration procedures have not been established for these instruments.

Wind Vanes

Mechanical wind vanes are frequently used in combination with cup or propeller anemometers to define the horizontal wind vector. A wind vane consists of a horizontal arm with flat plate assembly forming a sensor tail on one end and a balanced counterweight on the opposite end. The arm is mounted on a vertical post and is free to rotate. Wind flowing past the plate forces the vane into its most aerodynamically efficient (least resistance) position, with the plate downwind of the axis of rotation. The vertical post contains low torque potentiometers or photo-diodes to provide an analog voltage or digital output as a function of vane position. Vane position is converted to wind direction in degrees by a transfer function. Single potentiometer vanes operate from 0 to 360° in azimuth with a "dead spot" of about 5° in which data are lost. To overcome data loss, some vanes have dual potentiometers covering the ranges 0 to 270° and 270 to 540°. Alternatively, opto-electronic vanes use slotted discs mounted concentrically about the post to produce a series of binary counts for translation to wind direction. Other possible vane transducers include synchro motors and Hall effect

devices. Intercomparison tests of in-situ wind vanes (Finkelstein et al., 1986) indicate that comparabilities on the order of 5° for wind direction and 3° for wind direction standard deviation are possible. A reanalysis of the data by Lockhart (1989) suggests that intervane agreement to within 2° is possible.

Wind-vane performance characteristics include threshold, overshoot or damping ratio, and distance constant. These performance characteristics are defined by wind tunnel tests using ASTM-XXX1. Static bench calibration is verified by moving the vane through a series of positions defined on a jig where known outputs can be observed.

A variety of wind vane tail designs exist. These are the product of compromises between structural strength, vortex-shedding characteristics, and responsiveness. The design of a second-order mechanical system such as a wind vane involves a tradeoff between quickness of response and overshoot. Overshoot is defined by the distance constant and damping ratio (see glossary for definitions). A vane distance constant should be matched as closely as possible with its companion anemometer if the combined measurements are used for micrometeorological or diffusion modeling applications.

The wind-vane damping and distance constants are major design considerations, especially if vane-derived data are to be used to compute wind angle variances or standard deviations. Vanes must be damped to prevent excessive oscillations in turbulent winds. Manufacturers sometimes include electrical damping circuits in their wind vane transmitters to mask unwanted oscillations. Electrical damping does not compensate for inadequate vane design. Damping circuits should be bypassed during any evaluation of vane performance. The vane distance constant (the amount of air that must pass the vane before it responds to a change in wind direction) should be sufficiently small that it responds to the dominant scales of turbulent eddies at the height of measurement. In the surface boundary layer, the dominant eddy size scales directly with the height above ground. Table 2-1 includes recommended wind-vane characteristics for diffusion model applications.

Wind vanes are found in several different configurations and may include a front-mounted propeller. Some vanes are designed to include some motion in the vertical plane. These bidirectional vanes (bivanes) may also have a front-mounted propeller for wind-speed readings. Bivanes have limited mechanical response to vertical motion (usually $\pm 45^\circ$ to $\pm 60^\circ$), and the derived turbulence data are useful only when vertical motions do not drive the vane to its mechanical limits. Table 2-1 includes desirable bivane characteristics. While bivanes provide a relatively inexpensive means to obtain information on the vertical component of the turbulence field, their exposed horizontal

surfaces accumulate deposited material that unbalances the vane. When a bivane becomes unbalanced, its response characteristics change and its performance is degraded. As a rule of thumb, an out-of-balance condition in excess of $\pm 5^\circ$ indicates that the vane should be rebalanced. Bivanes are most suitable for micrometeorological applications at locations where they can be serviced on a daily basis.

As with mechanical anemometers, the sensor and moving components of wind vanes are subject to deterioration and wear. Wear creates shorts or dead spots in vane potentiometers. Additionally, wind-vane response is degraded as tails are damaged by exposure to field conditions. It is difficult to detect the onset of performance degradation in the field unless direct intercomparisons are made with other instruments. Mounting instruments at multiple levels on a meteorological tower not only provides extra data-points but also provides an opportunity to interchange instruments for performance verification. Periodic review of individual data-point scatter can reveal the occurrence of potentiometer dead spots. A simple field check to identify potentiometer faults consists of slowly rotating a vane through its range of angular positions while recording output. The recorded results should be free of spikes or dead spots.

Thermometers and Radiation Shields

Temperature measurements are made for a wide variety of purposes, and the application dictates the most appropriate type of thermometer to be used. For weather observing and climatological applications, low cost, simplicity, reliability, and long-term absolute accuracy are the most desired attributes. A good liquid-in-glass thermometer is appropriate for these applications. At the other end of the scale, measurements for temperature variance, heat flux, or temperature structure parameter (C_T^2) computations require fast response and short term relative accuracy. Fast-response hot-wire or sonic thermometers are most appropriate for these applications. Vertical temperature gradient computations require moderately fast response and high relative accuracy between probes. Quartz crystal, platinum wire, or thermocouple arrays are most useful for this application. Thermodynamic profiling requires good response and stability, wide-dynamic range, and low cost. Thermistors are often used for this purpose.

Most meteorological thermometers are of the immersion type, which require that the sensor absorb or emit energy to approach thermal balance with its surroundings. Thermocouple, thermistor, platinum-resistance thermometer (PRT), and quartz-crystal thermometers are examples of immersion thermometers. Immersion thermometers are susceptible to radiation effects. Their response times are governed by convective exchange of heat and are,

therefore, dependent upon wind-speed, probe geometry, and the thermal dissipation characteristics of the probe surface. Sonic and radiometric thermometers are free from these effects, but suffer from conversion uncertainties that limit their absolute temperature measurement accuracy.

Platinum Wire Platinum-Resistance Thermometers. The PRTs are based on a linear relationship between temperature and the electrical resistance of a metal wire of high chemical purity and thermal stability such as platinum. Platinum wire with a resistance of 100 ohms at 0 °C, increasing at the rate of nearly 0.4 ohms per degree Celsius ($\Omega/^\circ\text{C}$) is commonly used. The advantages of these PRTs include stability, repeatability, linearity, and excellent dynamic range. The PRT has been the traditional instrument of choice for maximum accuracy, stability, and reproducibility.

Major disadvantages of PRTs include small resistance change per degree Celsius, self-heating, and susceptibility of the low voltage signal to electromagnetic interference. Self-heating occurs as current passes through the PRT. Energy is dissipated as heat in proportion to the product of resistance and the square of the current. Self-heating bias can be minimized by selecting a large PRT with low resistance and a large thermal dissipation constant, but the tradeoff is slow response to temperature change. Fine-wire PRT probes can have response times on the order of tenths of seconds (s), but larger PRT probes with minimal self heating can have response times of several tens of seconds.

Large PRTs are favored when range and precision are more important than fast response. Industry standards and transfer functions for PRTs are well defined. Thin-wire PRTs are sometimes used for fast response measurements when absolute accuracy is not critical. Signal conditioning circuitry can be checked using a decade resistor box and the manufacturer's specifications. The PRT calibration is verified using thermal baths, as recommended in the Quality Assurance Handbook (1989). Large PRTs should be shielded from radiation and aspirated, but fine-wire PRTs used for fast-response temperature fluctuation measurements are often exposed without shielding. With careful attention to radiation shielding, circuit design, sensor matching, and calibration, PRTs are capable of measuring mean temperature difference and absolute temperature with resolutions of 0.01 and 0.05 °C, respectively (Stevens, 1967).

Thermoelectric Thermometers (Thermocouples). Thermocouples are simple temperature measurement devices made by joining two dissimilar metal wires. An electric current flows between junctions of two metals if a temperature gradient occurs in the wires. For small differences, the induced (Seebeck) voltage is

linearly proportional to the temperature differential. Typical output is 40 microvolts per degree Celsius ($\mu\text{V}/^\circ\text{C}$) for a copper-constantan thermocouple.

Thermocouples are used in a wide range of configurations and offer the advantage of being simple, rugged, and inexpensive. They can also be made with very thin wires for rapid response at the expense of ruggedness. Some disadvantages include a nonlinear, low voltage output and susceptibility to electro-magnetic interference and system biases. These errors include changes in wire characteristics during welding, decalibration because of wire age and mechanical or heat stress, and direct current (dc) offset acquired through the cabling or data acquisition system. In meteorological applications, thermocouples are frequently used for temperature difference measurements with a reference established at one level on a tower and junctions at other levels.

Precision thermocouple measurements are possible, but require special attention to noise, spurious voltage offsets, decalibration because of wire aging, and reference junction stability. A low signal level, on the order of 40 to 60 $\mu\text{V}/^\circ\text{C}$, creates a major problem for accurate temperature measurement. Requirements for accurate thermocouple measurements are described by Cheney and Businger (1990), who claim that accuracies near 0.01 $^\circ\text{C}$ are achievable. Thermocouple calibration involves matching of the transducers in thermal baths and checking the gain of the signal conditioner, as described in the Quality Assurance Handbook (1989). Fine-wire thermocouples have a large surface-to-volume ratio and dissipate heat quickly; thermocouple response time can be 0.1 s or better. Therefore, they can be used with a minimum of radiation shielding. The dynamic response of fine-wire thermocouples is described by Tsukamoto (1986).

Thermistors. The resistance of thermistors, which are made from metallic-oxide semiconductor materials, decreases with increasing temperature. Thermistors are inexpensive and provide moderate response (on the order of 10 s) for temperature profiling applications. Thermistor disadvantages include nonlinearity, self heating, aging, decalibration effects, and electromagnetic interference. Nonlinearity can be compensated for by software using a fitted polynomial transfer function. "Linear" thermistors, consisting of two thermistors in a sealed probe with compensation provided by external resistors, are also available. Mechanical aspiration of the sensor helps to minimize self heating, although the thermistor's slow heat dissipation rate remains a problem for accurate temperature measurements. Thermistor resolution is on the order of 0.05 $^\circ\text{C}$. Aging and decalibration upon exposure to high temperatures limit thermistor reliability. Thermistors are commonly used for temperature and temperature profile measurements when extreme accuracy is not critical. Luers (1990) describes thermistor temperature sounding

applications, which include a methodology for calculating radiation and conduction errors. Thermistors are also sensitive to stress produced by rough handling and mechanical vibration. Stress can produce hairline cracks in a thermistor's protective coating that alter calibration. To achieve maximum accuracy, thermistor calibration should include transducer matching at multiple data points in a thermal bath. Thermistors should be shielded and aspirated to minimize radiation and self heating effects.

Quartz-Crystal Thermometers. A quartz thermometer consists of a probe and oscillator circuit and a remote processing module that converts pulse counts to engineering units for input to a host computer. The physical principle underlying quartz thermometer operation is the temperature dependence of the resonant frequency of an electronic oscillator with a quartz crystal in its feedback loop. Depending on crystal cut orientation, the resonant frequency of the oscillator circuit can exhibit a temperature sensitivity of up to 100 parts per million (ppm)/°C. A stabilized reference oscillator allows precise (1 ppm or better) frequency measurement. The quartz crystal thermometer is beginning to displace platinum PRT as the standard for temperature measurement accuracy.

Because the quartz oscillator circuit frequency is stable and can be monitored with a high degree of precision, this measurement technique is characterized by a high degree of repeatability and low-drift rate. When coupled with an electromagnetic interference-free fiberoptic data link, this thermometer is capable of high accuracy temperature measurements (on the order of 0.01 °C). Oscillator frequency changes slowly with time, and quarterly recalibration is recommended to retain maximum accuracy.

The quartz probe assembly is susceptible to antenna effects, and oscillator power dissipation produces an unwanted heat source. However, these effects can be minimized through careful attention to probe and oscillator circuit design. The probes are sufficiently large that they must either be shielded or compensated for solar radiation effects. Quartz thermometers are most appropriate for micrometeorological applications where highly accurate temperature or temperature differential measurements are required. Figure 2-2 compares slow-response fiberoptic quartz and fast-response sonic thermometer measurements. The quartz thermometer's slow-response (on the order of 5 s) is accompanied by phase lag and smoothing.

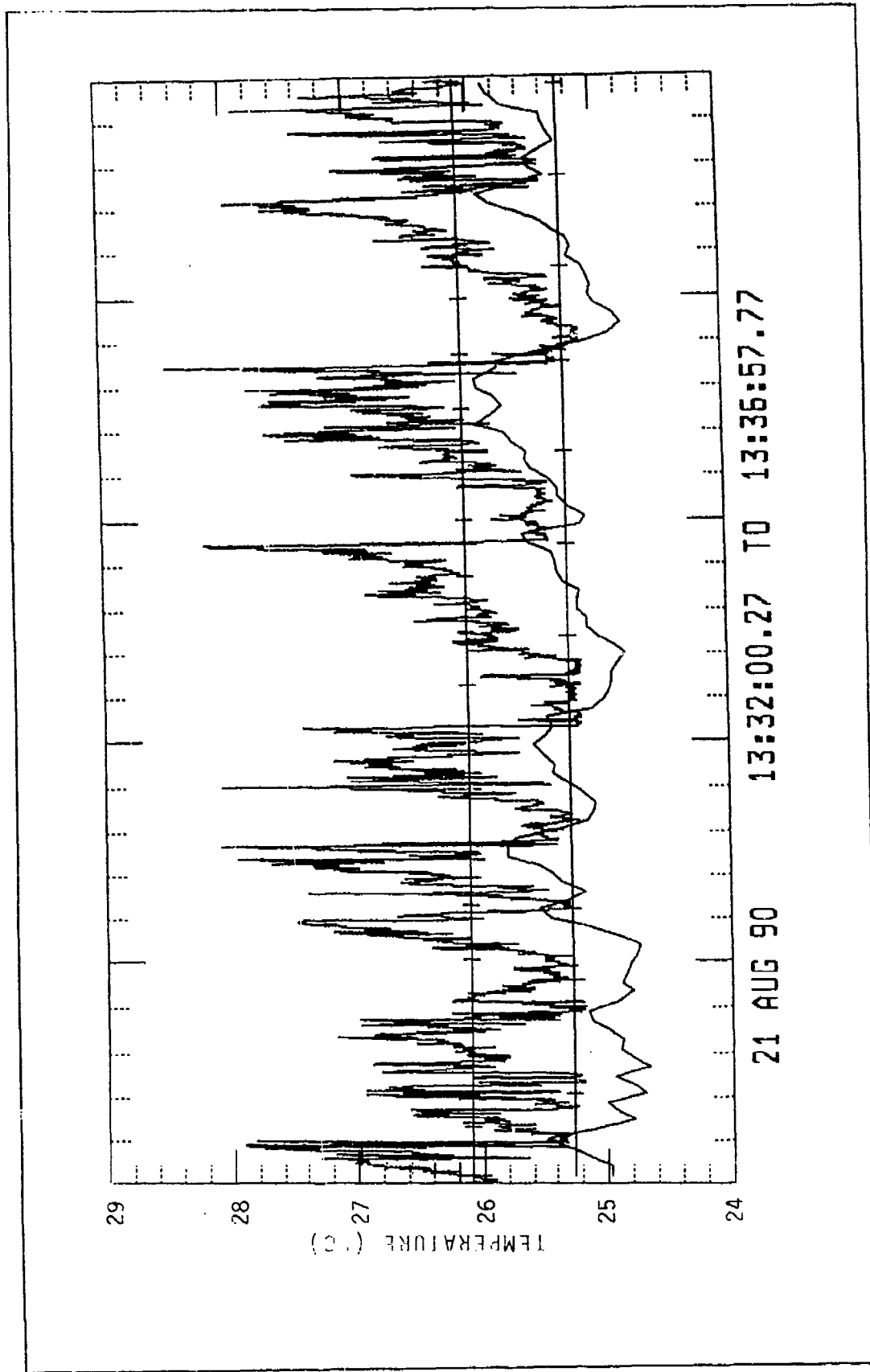


Figure 2-2. Near instantaneous response of a sonic thermometer (upper curve) and the slower response of fiberoptic quartz thermometer (lower curve).

Sonic Thermometer. In addition to wind component measurements, the sonic anemometer/thermometer can obtain speed of sound measurements which can be used to calculate the sonic temperature. Sonic temperature, closely related to virtual temperature (see glossary for definitions), is obtained from the speed of sound measurements by inverting the equation for acoustic propagation through air. Uncertainties in this inversion, because of variability of atmospheric constituents, (principally humidity) limit absolute temperature measurement accuracy to ± 1.6 °C (Biltoft, 1987). Consequently, sonic thermometry is not recommended for absolute temperature measurement.

Because acoustic wavefront propagation time rather than probe temperature is measured, the sonic thermometer is not susceptible to radiation effects. The speed of acoustic propagation across a short acoustic path also makes its response quasi-instantaneous. These characteristics are useful for heat flux and temperature variance computations where mean temperature and its bias are effectively removed, leaving a residual uncertainty of ± 0.03 °C (Biltoft, 1987). Fast-response sonic anemometer temperatures under convective conditions are illustrated in figure 2-2 along with the slower response of a fiberoptic quartz thermometer that provides a more accurate absolute temperature measurement. Sonic thermometer calibration is obtained using the method described in ASTM-XXX3, and operational practices are provided in ASTM-XXX2.

Radiation Shields. Immersion thermometers only report sensor temperature, which is a function of air temperature, but also includes radiation effects and conduction from attached surfaces. All immersion thermometers absorb solar and thermal radiation and emit thermal radiation. These thermometers contain metallic or metal-coated sensing elements of high-heat capacity whose absorptance and emittance are dominated by the characteristics of the sensor's surface finish or coating. Touloukian and DeWitt (1970) provide a compendium of radiative properties for metal surfaces. In contrast to metal surfaces, air readily transmits radiation and has a very low heat capacity. Fuchs and Tanner (1965) describe radiation effects on various types of thermometer surfaces. Thermometers are often shielded from radiation and aspirated to minimize radiation effects and maximize convective heat transfer from the air.

The design of a radiation shield to reduce direct radiation exposure while retaining a free flow of ambient air to the thermometer is almost as important as thermometer design itself when precise measurements are required. Shields come in two basic types: aspirated and nonaspirated. Aspirated shields, typically concentric tubes designed to reflect radiation, draw air across the instrument and exhaust it away from the intake. The constant flow rate in aspirated shields produces consistent thermometer exposure to the ambient air. Matched thermometer probes in

matched aspirated radiation shields can produce highly accurate relative air temperature measurements suitable for temperature gradient calculation. Well-designed radiation shields have aspiration rates on the order of 3 to 6 m/s and reduce radiation errors to ± 0.1 °C or less. Nonaspirated shields reduce radiation exposure but rely on ambient winds for ventilation. Because nonaspirated shields do not control air flow over the sensors, significant departures from ambient air temperature can occur during low-wind speed conditions. Nonaspirated shields are most suitable for instruments with small thermal mass such as fine thermocouple wires. Nonaspirated shields may be preferred at remote sites where available electric power is limited. They are not otherwise suitable for accurate temperature measurements. (Note: An ASTM Method describing the performance of radiation shields is being drafted.)

Liquid-in-Glass Thermometers. Liquid-in-glass thermometers use the thermal expansion of a liquid (usually mercury or alcohol) in a glass tube with a narrow bore as a means of measuring temperature. Mercury thermometers can be used with temperatures as low as -39 °C, while alcohol thermometers can be used with temperatures as low as -62 °C. These instruments are widely used for surface weather observations. Maximum and minimum temperatures are also conveniently taken with liquid-in-glass thermometers. As temperature increases, expanding mercury is forced past the constriction in the stem of a maximum-temperature thermometer. This constriction does not allow the mercury to return as the temperature decreases. An alcohol minimum-temperature thermometer contains a small dark index marker which is immersed in the alcohol but does not completely block the temperature bore. Surface tension moves the index down as the temperature decreases, but the liquid flows around the index as the temperature increases.

The accuracy of liquid-in-glass thermometers is a function of thermometer design and can be as high as ± 0.01 °C with a high quality mercury model. Thermometer glass changes slowly with time, and the liquid-in-glass thermometer scale may require adjustment every few years. Liquid-in-glass thermometers are calibrated by intercomparison against a reference standard in a thermal bath. Because liquid-in-glass thermometers are read manually, accuracy is primarily limited by the ability of the observer to resolve scale intervals.

Hygrometers

Water vapor is the most important constituent of the atmosphere for weather processes. It serves as a source and sink for great quantities of heat, and water vapor gradients determine cloud droplet growth and evaporation rates. Atmospheric water is found in solid, liquid, and vapor phases and exhibits extreme time and space variations. The unusual thermodynamic properties

of water make it difficult to measure except in bulk quantity. Definitions related to atmospheric water vapor content are presented in the glossary. Instruments commonly used for water vapor sensing measure one of the following: (1) wet-bulb and dry-bulb temperatures, (2) relative humidity, (3) dew point, or (4) water-vapor concentration. Important considerations in choosing any water-vapor measurement system are the ranges in humidity and temperature for operation and the environmental contamination to which the instrument is exposed. Operation beyond the design range or in a contaminated environment will degrade measurement quality and possibly destroy the sensor. Relative-humidity measurement accuracies of ± 5 percent or dew point measurement accuracies of ± 1.0 °C are generally sufficient for most applications. However, fast response and high accuracy are sometimes required to define water vapor effects on wave propagation, especially in the infrared through radio wave portion of the electromagnetic spectrum. Wiederhold (1975) describes humidity measurement techniques, gives guidelines for instrument selection, and provides comparison of available humidity sensors.

Lithium-Chloride Dew Cell. A commonly used saturated salt dew point sensor consists of a lithium chloride (LiCl) coated fabric bobbin containing electrodes. An alternating current passes through the salt coating to produce resistive heating. Heating causes evaporation from the hygroscopic LiCl solution with the rate of evaporation controlled by vapor pressure. As the bobbin loses water, resistance of the LiCl decreases. The bobbin cycles through heating and cooling until equilibrium with the atmospheric vapor pressure is reached. The equilibrium temperature is used as a measurement of ambient dew point with an accuracy near ± 1 °C over a temperature span from -12 to +38 °C. The instrument operates within a range of 11 to 95 percent relative humidity, but performance declines markedly at humidities below 20 percent (Henning, 1971). The LiCl sensor is a low cost, rugged, slow responding, moderately accurate instrument when operated within its limitations. It is less sensitive to contamination than adsorption/desorption humidity sensors. Response is slow (dew cell response time is typically several minutes) because of bobbin thermal mass and the heating/cooling cycles. Consequently, averaging readings over a 15-minute period is recommended. The sensor should also be operated within an aspirated radiation shield. Exposure to water or excessive contamination will ruin the bobbin coating. Once set into operation, the instrument should be run continuously to prevent moisture accumulation from disturbing the LiCl coating. However, recoating is a simple procedure easily accomplished in the field and should be done weekly to minimize contamination effects. Folland (1975) provides a guide to the use of dew cell hygrometers. Measurement accuracy can be verified in a temperature-humidity chamber, and field performance can be verified using a chilled-mirror hygrometer as a transfer standard.

Chilled-Mirror Hygrometers. Optical condensation hygrometers measure dew point by thermoelectric (Peltier) cooling of a polished mirror surface until condensation occurs. Dew formation on the mirror interrupts a light beam to shut off the cooling process. A thermometer embedded in the mirror surface measures the dew point. These instruments are capable of faster response and operation over greater temperature and humidity ranges than most other hygrometers designed for field use. Dew-point measurement range is typically -70 to +60 °C. The dew-point hygrometer also serves as a secondary laboratory standard.

Optical condensation hygrometer response is limited by the finite amount of time required to condense or evaporate a film on the controlling mirror surface. Accuracies of ± 0.5 °C or better are possible. Operator adjustments for the "gain," "compensation," and "thickness" affect instrument performance. Gain controls the system dynamic response, while compensation is a phase lead to the amplifier circuit to compensate for the phase lag of the Peltier cooler. Compensation dampens oscillations to allow a higher gain setting and improved dynamic performance. Thickness controls the depth of film on the mirror before cooling is interrupted. The thickness adjustment offers a compromise between fast dynamic response and insensitivity to mirror contamination. Skill and patience are needed to optimize these adjustments, although microcontroller technology has recently been used to automate this adjustment procedure (Richner et al., 1991). The ASTM-D4230 (1989) presents a procedure for measuring humidity using a chilled-mirror hygrometer.

The cooling rate of the Peltier cooler in an optical condensation hygrometer is rapid, usually within seconds; however, settling time is inversely proportional to vapor pressure. For very low vapor pressures (usually associated with temperatures below -18 °C), the small amount of water vapor present requires several tens of minutes to form the required condensate thickness on the controlling mirror. In spite of the increased time constant, the optical condensation hygrometer produces useful data at cold temperatures where most other humidity instrument response is poor. An additional complication at temperatures between 0 and -30 °C is that either dew or frost may form on the mirror surface. The possibility of accumulating either dew or frost creates a measurement ambiguity unless freezing is artificially initiated on the mirror.

The mirror surface of the optical condensation hygrometer is relatively insensitive to contamination, although cleaning every 2 or 3 days is recommended in a very dusty environment. Mirror self-cleaning procedures are generally ineffective in high-dust concentrations. Hosom et al., (1991) experienced some success

with cleaning water soluble contaminants off the mirror in a marine environment, although oils and grease accumulations remain a problem. Dirty mirror surfaces can cause the equipment to oscillate about the condensation point.

Disadvantages of optical condensation hygrometers include cost; complexity of electronics; the requirement for manual optimization of gain, compensation, and thickness; and condensation in the sensor cavity during high moisture conditions. The size and power requirements of the instrument also limit its applicability for remote site micrometeorological measurements, although these instruments are often used as transfer standards for checking other humidity instruments.

Adsorption Hygrometers. Other common humidity sensors electrically measure the percent relative humidity. These sensors operate on the basis of changes in conductivity, capacitance, or resistance because of adsorption or desorption of moisture as humidity changes. They typically operate over a humidity range of 10 to 98 percent. Soluble salts, halogens, or any substance that alters surface resistivity can decalibrate or destroy this type of sensor. These instruments should not be used in highly contaminated environments. If temperature-compensated and mounted in an aspirated radiation shield, these instruments can produce accuracies of ± 5 percent over a limited range of temperatures. A pilot study by Muller and Beekman (1987) revealed major accuracy problems at cold (-20 °C) temperatures for most instruments of this type. Hosom et al. (1991) discovered significant calibration drift and sensor failures for adsorption hygrometers operated in an adverse marine environment. Calibration procedures vary with instrument design but most include two or three humidity points (20, 50, and 80 percent). Some instruments exhibit noticeable hysteresis effects, particularly following long exposure to saturation.

Lyman- α Hygrometers. The Lyman- α hygrometer offers a fast-response, fine-scale humidity fluctuation measurement capability. Instrument operation is based on Beer's law absorption by the hydrogen constituent of water molecules at the Lyman- α (121.5-nm) wavelength. The sensor consists of a glow discharge tube and a detector tube connected to an electrometer circuit, with the detector set behind a magnesium fluoride window. Lyman- α operating principles are described by Buck (1985). A gap of 0.5 to 2 cm between the source and detector offers fine spatial resolution at the expense of significant flow distortion effects (Wyngaard, 1981). The window is sensitive to etching and contamination, making the Lyman- α subject to rapid calibration drift. Consequently, the Lyman- α hygrometer is often used in conjunction with a slow-response reference instrument such as a

chilled-mirror hygrometer. Lind and Shaw (1991) describe techniques for adjusting Lyman- α calibration during airborne measurement applications, and Priestly and Hill (1985) describe ground-based applications. Cost and maintenance considerations limit this instrument to research applications.

Infrared Hygrometers. Fixed-point humidity or dew point sensors are limited by the requirement for an interaction between water vapor and a solid surface through relatively slow acting processes such as condensation, adsorption, and cooling. Fast response optical humidity sensors use closely-spaced, columnated beams of infrared light and a differential absorption technique to measure absolute humidity. These instruments have a transmitter which sends out two parallel beams closely spaced in frequency but with different water vapor absorption characteristics. At the receiver end, the ratio is formed of the energy received from the absorbing and non-absorbing beams. This ratio is proportional to the absolute humidity (grams per cubic meter) in the sampled volume. With sealed optics and non-reactive sensor plates, optical humidity sensors are relatively insensitive to contamination, capable of operation at extreme temperatures without degradation, and provide accurate data at high data rates. Internal calibration checks minimize calibration drift. The major disadvantage of this type of instrument is the tradeoff between sensitivity and expense. Functional precision of these instruments has not been determined, but should be 0.05 grams per cubic meter (g/m^3) or better. Fast response humidity instruments of this type can be used for moisture flux measurements. Calibration can be verified on some models by inserting optical glass with known absorption characteristics between the transmitter and receiver.

Psychrometers. Psychrometers consist of two matched thermometers mounted together in a holder. One thermometer bulb is exposed to ambient air conditions (the dry-bulb) and the other is covered by a wet muslin sock (the wet bulb). When the thermometers are aspirated, evaporative cooling of the wet bulb lowers its temperature. The dry bulb-wet bulb temperature difference is known as the wet-bulb depression. Standard meteorological tables relate dry bulb temperature and wet bulb depression to relative humidity and dew point. Some psychrometers have been automated but most are used manually. Psychrometers can provide very accurate dew point and humidity readings for temperatures above 0 °C and high humidities. At low humidities, a significant amount of energy must be dissipated by evaporative cooling for the wetbulb to reach equilibrium. At this point, the aspiration rate becomes a crucial limitation on accuracy. At temperatures below 0 °C, the wet bulb can be either liquid or frozen, each with unique thermodynamic equilibrium values. Other factors limiting accuracy include cleanliness of the muslin sock, water purity, and effects of water temperature on wet bulb readings.

Accuracy is a function of the care with which the wet bulb reading is taken and the ability of the observer to resolve the thermometer's temperature scales. Dynamic response of a psychrometer is slow; psychrometric techniques are most applicable for mean humidity measurements. The dynamic response of a fine-wire psychrometer used for water vapor flux measurement is presented by Tsukamoto (1986).

While most psychrometers are hand operated, some automated versions are in use. Tests of automated psychrometers indicate agreement to within 10 percent relative humidity for most conditions (McCaughey et al., 1987). Hosom et al. (1991) found psychrometers to be repeatable to within 0.5 °C (dew-point equivalent) and accurate to about 0.5 °C, providing the most reliable measurements currently available in adverse marine environments. Maintaining a properly wetted wick is a major problem for automatic psychrometers. Procedures for use of psychrometers are described in the WMO Guide (1983).

Hair Hygrothermograph. Perhaps the most basic humidity instrument is the hair hygrothermograph. This instrument mechanically links human hair to a pen. Hair length increases with humidity. The pen leaves an ink record on a recording chart mounted on a clock-driven rotating cylinder. The hygrothermograph is a simple, inexpensive way to obtain a week's analog record of relative humidity. Disadvantages of the hygrothermograph include slow response time, a requirement for manual chart reading, and limited accuracy. Hair exhibits a strong hysteresis effect and, when exposed to high humidity, will not return completely to low humidity calibration positions. Also, hair characteristics change over time and with exposure to contaminants. At best, calibrations are approximate because of hair's highly nonlinear response. Hair hygrometers are reasonably accurate only in conditions where humidity changes over a limited range. Hair hygrometers and their applications are described in the WMO Guide (1983).

Barometers

Pressure can be measured directly on-site or calculated using measurements from a nearby weather station. The horizontal pressure gradient is typically several orders of magnitude less than the vertical pressure gradient. Therefore, pressure can be easily calculated for a remote site using the pressure measurement at an established weather station and the hypsometric equation, given the height difference and an estimate of mean layer temperature.

Pressure readings can be obtained from mercury-in-glass barometers, aneroid barometers, or digital barometers. Mercury and aneroid barometers are common in weather stations where they remain in a controlled atmosphere (temperatures close to 20 °C).

The mercury barometer operates on the principle of air pressure forcing the mercury column up an evacuated tube. Barometers are usually read to the nearest 0.1 millibar (mb). Barometric pressure measurement is described in the WMO Guide (1983).

Mercury Barometers. First-order weather stations often maintain mercury barometers as a pressure measurement standard. These instruments can be highly accurate but must be mounted on a stable, vibration-free platform in a temperature-controlled room. Mercury barometers require local gravity correction and capillary corrections. Neither mercury nor aneroid barometers are particularly well suited for field measurements. A hypsometric calculation using pressure from a nearby weather station is usually preferable to carrying one of these instruments into the field.

Aneroid Barometers. The aneroid barometer works on the principle of expansion/contraction of an evacuated cylinder because of atmospheric pressure change. An aneroid barometer is read directly from a dial attached to the cylinder. Aneroid barometers have no gravity error because they are not weighing devices, but do have a small hysteresis error because of metal elasticity. Pressure readings for weather observations are usually taken at hourly intervals, so instrument response time is not critical. The barograph is another aneroid pressure device. The barograph consists of a chart mounted on a clock-driven drum, which is marked by a pen connected to the aneroid cell. Barographs are used to keep an analog record of pressure tendency. Barographs and aneroid barometers are usually checked annually against a standard mercury barometer. Aneroid barometers are less sensitive to temperature and vibration than mercury barometers, but are most accurate if kept in a controlled environment and not subjected to spurious pressure changes caused by opening and closing exterior doors. Garratt et al. (1986) report on root means square (rms) noise of 0.06 mb and a mean absolute drift of 0.2 mb per year for an electrical-readout aneroid barometer maintained at constant temperature.

Digital Barometers. Recent developments in barometry include temperature-compensated digital barometers. These microprocessor-controlled devices can provide accuracies to within ± 0.3 mb over a temperature range of +5 to +55 °C, which is a sufficient accuracy for most applications. Digital barometers are usually checked annually against a standard mercury barometer. Calibration over the instrument's full range is performed in a pressure chamber with corrections programmed into the instrument or a data logger.

Precipitation Sensors. Precipitation type, rate, areal extent, duration, and accumulation have a profound effect on the fate of airborne material. Standard rain gages are relatively crude devices which provide only gross precipitation estimates.

However, these devices can be of use for long-term monitoring programs. Far more relevant to model input needs are new optical precipitation sensors which provide real-time measurements of the type, rate, and duration of precipitation. Rain gage network and radar rainfall measurement biases and error variances can be estimated using complementary sets of rain gage and radar rainfall rate data (Barnston, 1991).

Mechanical Gages. The two standard types of precipitation measuring devices are the tipping bucket and weighing rain gages. The tipping bucket gage collects liquid water in a cylinder which funnels it into one of two small buckets mounted on a fulcrum. When the upward tilted bucket collects the equivalent of 0.01 inches of water, its weight overcomes the eccentric counterbalance and it tips down, emptying its contents. The cycle then repeats for the other bucket. Each tipping of the bucket is recorded on an analog or digital recorder with respect to time. Precipitation rate is estimated from the number of tips per unit time. The weighing precipitation gage consists of a funnel which pours accumulated precipitation into a bucket mounted on a scale. The change in weight is recorded on a gear-driven drum recorder.

The tipping bucket and weighing gages require careful site selection to optimize performance. They are most accurate in light winds. Strong, gusty winds vibrate the gages, causing erroneous readings. Strong winds also blow precipitation horizontally across gage openings, creating a wind induced loss of 10 to 20 percent (Lindroth, 1991). Consequently, rain gage sites should be chosen where wind effects are minimized without the gage being shadowed. These gages also become less accurate in heavy precipitation because of splashing, and they may require heating in locations where snow or ice accumulation occurs. Mechanical gages are marginally suitable for precipitation rate measurements over time periods shorter than 1 hour. Procedures for precipitation instrument placement and event measurements are covered in the WMO Guide (1983).

Optical-Precipitation Sensors. The limitations of the standard precipitation gages have driven the development of the light emitting diode (LED) weather identifier. This optical device consists of an LED transmitter and receiver which distinguishes precipitation type, intensity, duration, and accumulation with fast-time resolution. The optical gage is unencumbered by the limitations imposed by the standard gages and is being tested by the National Weather Service for use at their modernized weather stations. An optical instrument designed to measure the size and concentration of raindrops is described by Illingworth and Stevens (1987).

The most basic optical precipitation sensors measure only the intensity of precipitation. Some models are designed for permanent installation with available commercial power, while others are battery powered (± 12 V) and are suitable for remote or portable applications. Care must be taken that the instrument is level and that the receiver does not receive direct sun. A calibration device is available for the Scientific Technology Inc., model 705 optical precipitation sensor and is being developed for their portable model. Optimum sampling time for these instruments is 5 s.

CHAPTER 3

ACTIVE REMOTE SENSING INSTRUMENTS

Advances in electronics, sensor technology, and wave propagation theory have led to the development of remote sensing meteorological instruments. These instruments typically obtain information from a forward- or backscattered electromagnetic or acoustic signal emitted by the instrument's transmitter. A major advantage of remote sensing is that the classic problem of an instrument's size or thermal mass interfering with the measurement is eliminated. Also, remote measurements obtained along a propagation path can offer temporal and spatial resolution advantages and can be more appropriate for some applications than measurements made at a single point. Remote measurement paths can be horizontal, slant range, or vertical. In some cases, remote sensing may be the only means of making measurements at inaccessible sites.

Disadvantages of remote sensors include the technical competence required to operate the equipment and interpret the results, the relatively high cost of the instrumentation, and the absence of absolute performance standards. "Accuracy" is not defined for these instruments because the return signals cannot be directly related to the measured variable through transfer functions as with many point sensors. Instead, the signals are typically processed through a series of mathematical filters, transformations, and analysis routines. Remote sensor output should, therefore, be viewed as an interpretation of the signal rather than a measurement that can be traced to a standard reference. Consequently, remote sensor performance is often characterized by bias, comparability, and precision estimates derived from instrument intercomparison studies (see chapter 6).

Remote sensors rely on assumptions about the scattering medium, and errors occur when these assumptions are violated. For example, a ground-based wind profiler uses multiple-path measurements to resolve the three orthogonal components of the wind vector (east-west, north-south, and vertical). These measurement paths are often not collocated. Construction of a wind vector from wind components along three separate paths requires the assumption of homogeneity between the paths and use of time averaging to minimize errors that occur when the wind field sampled in one beam varies from the wind field sampled in another. Lenschow (1986) discusses active remote sensor applications and limitations.

Doppler-Acoustic Sounders

Monostatic Doppler acoustic sounders (sodars) are ground-based remote sensing instruments that use the acoustic Doppler effect to measure wind and turbulence profiles above the sodar antenna array. The most common sodar configuration includes a three-antenna array mounted on a trailer with one antenna transmitting acoustic energy directly above the array (the vertical axis) and the other antennas tilted 15 to 18° off the vertical axis and at orthogonal directions to one another. This arrangement permits wind measurements made along the antenna radial directions to be resolved into the vertical, north-south, and east-west wind components. These wind components are then converted into wind speed, wind direction, and turbulence data. A more recent sodar design consists of a phased array of small acoustic transmitter-receivers where beams are electronically steered along desired radial directions.

Sodars use the Doppler shift of backscattered acoustic energy as a means of obtaining wind and turbulence measurements. A measurement cycle begins with the transmission of acoustic pulses from compression drivers within one of the tuned directional antennas. After transmitting, each antenna sits for several seconds in a listening mode to receive backscattered signals. The transmitted acoustic energy propagating along a radial direction encounters thermal inhomogeneities in the atmosphere which scatter the energy, a small portion of which is backscattered to the antenna of origin. Each return signal is characterized by its intensity, Doppler frequency shift, and spectral width. The arrival of each signal is also time tagged. The time interval between transmission and reception, multiplied by the speed of sound and divided by two (to account for the round trip out from and back to the antenna), identifies the radial distance at which the scattering occurred. The Doppler shift in the return signal's acoustic frequency indicates the speed and direction of air motion along the radial axis. The frequency is shifted towards a higher frequency if the scattering volume is moving toward the antenna and towards a lower frequency if the scattering volume is moving away from the antenna. Signal processing techniques are used to assess data quality and to remove noise. Additional software converts the returned signals into vertical profiles of wind and turbulence. Acoustic propagation theory and remote wind sensing are described by Brown and Hall (1978) and Lenschow (1986).

Commercial sodars consist of one-beam, three-beam, or phased array designs. The antenna for each beam consists of an enclosure, a parabolic reflector, and transducers. The enclosure is lined with sound absorbing foam to minimize reception of background noise. The reflector and enclosure form a focused acoustic beam and the transducers generate and receive acoustic

energy. Antennas may contain heaters to melt snow as it accumulates in the enclosure. The one-beam sodar samples along the vertical axis, while the three-beam design samples along the vertical and tilted axes. The primary use of a single-beam sodar is to obtain the boundary layer stability structure for estimates of the mixing depth, although acoustic sounder height range is often insufficient for this purpose. Three-beam and phased array sodars can resolve both the vertical and horizontal components of the wind.

Sodar range is a function of transmitted pulse energy, antenna gain, acoustic frequency, pulse repetition frequency, ambient noise, and atmospheric conditions. Most sodars are designed to provide wind profiles from 60 to 600 m above ground level, and occasionally higher as conditions permit. Ringing of the compression drivers limits the near-surface echo return, while background noise and decreasing return signal strength with height limit the height range. Pulse repetition frequency determines the length of the listening mode between pulses. Selection of a pulse repetition frequency is based on desired sampling height. Each sampled volume is a cylindrical section of the atmosphere, typically 30 m deep with a diameter defined by the antenna beamwidth. The effects of sodar design, spectral broadening, and atmospheric refraction on sodar performance are discussed by Spizzichino (1974).

Sodars can be trailer mounted for mobility or mounted on fixed pads. In either case, careful consideration must be given to the operating environment. Sodars are sensitive to noise sources and should not be located near variable-speed electrical motors such as fans. Noise from road or airport traffic also degrades performance. Conversely, acoustic pulses generated by the sodar can cause complaints from people living or working nearby. Acoustic waves are reflected by solid objects such as nearby buildings or towers. Because the intensity of echo returns from stationary solid objects often exceeds the intensity of atmospheric returns, care must be taken to avoid siting sodars near large reflecting surfaces such as tall buildings. Also, acoustic signal levels are low, and unamplified voltages produced by these signals are correspondingly low. Consequently, sodar data cables must be shielded from electrical interference. Each manufacturer has proprietary programs designed to separate noise from the return signal and to compute wind components.

The principal advantage of sodars is that they can provide a continuous wind and turbulence profile record over a significant portion of the surface boundary layer. Sodar monitors and controls can be operated from a centralized facility via communication lines while the antennas are stationed at remote locations. Sodars operate under most weather conditions, but the noise from heavy rain, hail, and strong winds degrade system performance. Strong horizontal winds (on the order of 15 m/s) can also deflect

the acoustic beam and cause loss of signal. The sodar components most prone to failure are the compression driver diaphragms, which are typically replaced annually. System performance also decreases as the sound-absorbent foam lining the antennas degrades because of mechanical abrasion, dirt accumulation, and ultraviolet light exposure.

Sodars offer a cost-effective monitoring capability for winds within the first 500 m of the earth's surface. They do not obstruct airflow in the measured volume or create aircraft hazards. However, low background noise requirements and the size of the horn enclosures (typically 1.5 to 2 m in diameter) often make site selection difficult near industrial or residential areas. Another problem is associated with sampling volume separation. For a trailer-mounted sodar, the north-south horn, the east-west horn, and the vertical horn have separate sampling volumes. Temporal averaging of 15 minutes or longer is assumed to satisfy spatial homogeneity requirements over these sampling volumes for horizontal wind computation. A compendium of sodar applications has been compiled by Singal (1988).

Sodar performance validation procedures have been developed (Baxter, 1991). These procedures include verification of electronic timing, range-gate intervals, and wind calculations. Also included in the procedure are external factors such as sound-level readings, alignment checks, grounding, and cabling. Intercomparison checks are made with wind data from a reference system such as a tethered balloon.

Sodar performance is strongly influenced by stability of the atmosphere, with increasing uncertainty in wind measurements during unstable conditions. A number of field intercomparisons of acoustic sounder data with data from radiosondes, tether-sondes, and tall meteorological towers have shown that during favorable operating conditions sodar wind profiles averaged over 15-minute periods compare well with wind measurements derived from other systems. Typical functional precision under these conditions is on the order of 1 m/s for wind speed and 30° for wind direction (Finkelstein et al., 1986). Turbulence data computed from sodar wind measurements have had mixed results. Sampling volume size, beam divergence, low-sampling rates, and variable degrees of correlation between horizontal and vertical wind components detract from the sodar's potential as a turbulence instrument. Intercomparison test results indicate that sodars have a marginal capability for defining vertical velocity variance and virtually no utility for horizontal wind angle variance measurement (Biltoft, 1991). The sodar's primary application is as a cost-effective alternative to tall meteorological towers for wind profile monitoring.

An alternative to the monostatic sodar is a bistatic configuration, which consists of a transmitter and a set of remote receiver antennas. The main advantage offered by bistatic configurations is improved return signal strength because of scatter from velocity as well as thermal inhomogeneities. The requirement for remote receiver antenna arrays limits bistatic applications to fixed sites with sufficient operating space available. Few bistatic sodars are commercially available.

Radar-Wind Profilers

Radar wind profilers are ground-based, phased-array radars that obtain vertical profiles of wind from radio-wave energy that is Doppler shifted and backscattered from patches of turbulence. Measurements derived from beams oriented along 3 to 5 radial directions (typically vertical and 15° off vertical towards east-west and north-south) are resolved into vertical, east-west, and north-south wind components. These components are then converted into wind speed and direction data. Profiler operation is described in the National Oceanic and Atmospheric Administration/Environmental Research Laboratory (NOAA/ERL) Profiler Training Manual #1 (van de Kamp, 1988), and by Peterson (1988). Doviak and Zrnic' (1984) provide detailed descriptions of radar operation and signal processing for meteorological applications including turbulence measurement, clear-air profiling, and weather echo interpretations.

The atmosphere is in a continuous state of change as patches of air with different temperature and moisture content are continually created or dissipated. A portion of the radio-wave energy transmitted through the atmosphere by a radar is backscattered from these turbulent patches towards the radar's receiver. The backscattered signal from each pulse arriving at the radarreceiver is usually so weak that it is below the receiver's noise threshold. However, if a number of radar returns are added together, the sum of the backscattered signals increases while the sum of the random noise decreases towards zero. Consequently, when a sufficient number (many thousands) of radar returns are averaged, a detectable composite signal emerges through the noise. Data processing algorithms are used to define the signal peak and signal-to-noise ratio.

Backscattered signals are characterized by their intensity, Doppler-frequency shift, and spectral width. Each returned signal is also time tagged. The time interval between transmission and reception, multiplied by the speed of light and divided by two (to account for the round trip out from and back to the antenna), identifies the radial distance (range) at which the scattering occurred. Backscattered radio-wave frequencies are Doppler shifted in proportion to the velocity along the radial axis of the turbulent patch responsible for the scattering. The shift is towards a higher frequency if the scattering volume is

moving towards the antenna and towards a lower frequency if the scattering volume is moving away from it. Spectral width is a data quality indicator because it shows the spread of velocities averaged into the returned signal. Signal-processing algorithms assess data quality and convert the Doppler-shifted returns from the vertical and off-vertical radial directions into vertical profiles of wind speed and direction.

Radar performance is determined by atmospheric reflectivity (η), radar characteristics, range to the target (r), and range resolution (Δr). Key radar characteristics include the power-aperture product ($P_t A_e$), pulse length (τ), wavelength, and bandwidth. The choice of a specific set of radar characteristics depends on the wind profiling application. Gossard and Strauch (1983) define clear air radar performance in terms of back-scattered signal power (P_r)

$$P_r = 0.0354 P_t A_e \tau \eta \Delta r / r^2 \quad (3-1)$$

For Bragg scatter, reflectivity is primarily determined by the strength and scale of the scattering medium and the available bandwidth from which to draw the reflected signals. Reflectivity tends to decrease with height above the surface in proportion to atmospheric density. The scale of the most efficient scatterers ranges from 10 cm at a few hundred meters above the surface to several tens of meters in the mesosphere (Balsley, 1987). These scale and intensity considerations suggest the use of shorter radar wavelengths for low-level profiling and longer wavelengths for profiling through greater heights in the atmosphere.

Principal radar performance parameters include transmitted power (P_t), effective aperture (A_e), and pulse length. The product of P_t with A_e is the power-aperture product, which determines a radar's power transmission capability and sensitivity to returned signals. The decrease in η with height dictates a larger $P_t A_e$ for greater height ranging. Pulse length determines the range resolution or length of the range gate. Short-pulse lengths provide fine-range resolution but limit range because of limited transmitted power. Pulse coding is sometimes used to maximize power and range resolution.

A major radar engineering compromise must be made between system cost and the need for long-range and fine-range resolution. Received power at a given range and Δr are both proportional to τ . Therefore, to increase range resolution (decrease Δr) without sacrificing received power, $P_t A_e$ must be proportionally increased. Because radar costs increase with $P_t A_e$, cost factors limit a radar's range and range resolution. Given these (and many other) engineering considerations, wind profiling within the first 5 km of the earth's surface can be accomplished

with small, mobile, inexpensive profilers operating at radar wavelengths of 10 to 33 cm. Full tropospheric profiling with a 10- to 15-km range can be reasonably done at wavelengths of 67 to 74 cm. Some profilers of this type can be moved from one site to another. Profilers operating at 50 MHz (6-m wavelength) with very large antenna arrays are designed for fixed-site profiling through the stratosphere and mesosphere. Table 3-1 summarizes the three main types of wind-profiling radars and their characteristics.

TABLE 3-1. TYPES OF WIND-PROFILING RADARS					
Profiler Type	Typical Range (km)	Range Resolution (m)	Operating Frequency (MHz)	Antenna Size (m ²)	Mobility
Boundary Layer	0.1 - 5	30 - 150	915 - 1300	10	Mobile
Tropo-spheric	0.5 - 16	250 - 1000	404 - 450	100	Trans-portable
Strato-spheric	2 - 60	150 - 1000	50	10000	Fixed

An important radar wind-profiling consideration is frequency allocation. Profiling radars transmit considerable power and require significant operating bandwidth. The radio-frequency spectrum is already allocated, so wind profilers must fit into a crowded portion of the electromagnetic spectrum. Existing 404-MHz profilers currently share a frequency band also used for meteorological aids and search-and-rescue satellites (SARSAT). Because of possible interference with SARSAT beacons, these profilers are programmed to cease transmission when a SARSAT passes overhead. Profiler operation requires approval through frequency management offices.

Advantages of a radar wind profiler include continuous operation and automated data processing. Continuous operation provides wind profiles with a temporal resolution unattainable from balloon-borne measurement systems. Automated data processing makes the data available soon after the end of the data

collection period and requires no manual intervention. Also, profilers can operate in most weather conditions and require no expendable flight equipment. Most important, computer-based profiler operation requires no on-site personnel; an entire profiler network can be controlled by a single operator stationed at a centralized location. Radar wind profilers offer greater height ranging capabilities than sound ranging remote sensors (sodars), and coherent averaging of returned signals provides noise suppression and signal enhancement unavailable for sodars and lidars.

Profiler functional precision is estimated to be between 1 and 2 m/s, comparable to the best radiosonde precision (see Free Balloons, chapter 5). Performance verification techniques are under development, and improvements in profiler data processing algorithms are expected to continue through the 1990s. Profilers provide data at 5- or 6-minute reporting intervals or multiples of these intervals. These reporting intervals are sufficiently frequent to provide details of transient features (wind shears, downbursts) in the atmosphere that are usually missed by balloon-borne measurement techniques. Profiler data can be useful for real-time monitoring of the winds affecting the transport and diffusion of rocket exhaust plumes or other large-scale or continuous sources. During an evaluation of 3-beam ultra high frequency (UHF) profilers, Strauch et al. (1987) found the horizontal wind component error to be normally distributed with a standard deviation of 1.3 m s^{-1} . Using only data with high signal-to-noise ratios, the error standard deviation was reduced to 0.9 m s^{-1} . Theoretical profiler precision is several tens of centimeters per second, and profiler measurement precision will likely improve as better data quality control algorithms are developed. A typical wind profiler data display is presented in figure 3-1.

Scintillometers

A scintillometer is a ground-based, remote-sensing instrument designed to measure crosswind components and optical turbulence intensity along a line-of-sight path established between a transmitter and a downrange receiver. Scintillometer hardware includes a laser or LED light source and diffusing optics in the transmitter and optical receiver. The transmitter and receiver are separated by a distance of 200 m to several kilometers. Two basic scintillometer designs currently exist: finite-aperture and spatially averaged filter.

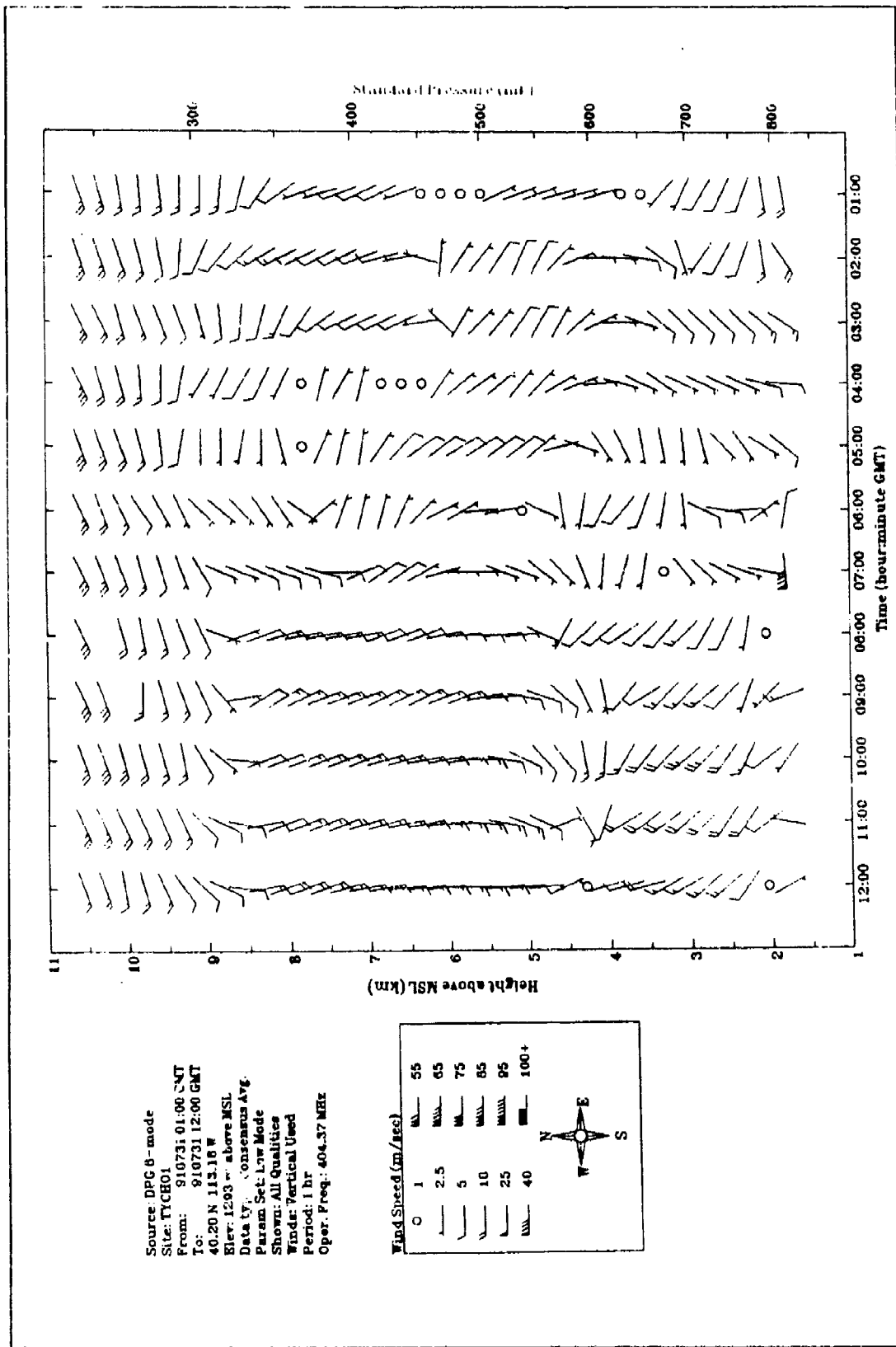


Figure 3-1. Hourly consensus data from the Dugway Proving Ground radar wind profiler.
 (Source: Wang et al., (1991).)

Techniques for using atmospheric turbulence-induced scintillation to derive path-averaged refractive index and transverse wind measurements were developed by Lawrence et al. (1972) and Clifford et al. (1974). Scintillometer operation is based on the principle that scintillations or light intensity variations occur as atmospheric density discontinuities create refraction effects (phase shifts) in light propagating along a path. The phase shifts cause light rays to scintillate (reinforce or cancel) as they arrive in phase or out of phase at a receiver position. Refraction effects from different portions of the path contribute to the total scintillation pattern. The refractive index structure parameter CN2 is related to the received scintillation: the logarithmic intensity variance in irradiance (radiant flux received per unit area) at the receiver aperture. The scintillometer cross-path wind component is obtained by calculating the time delay for characteristic scintillation patterns to drift between parallel beams. Cross-beam translation speed is calculated using the known separation distance between optical paths and a time delay determined from analysis of the autocovariance of irradiance from aperture pairs.

A number of scintillometer deployment configurations are possible. The simplest is a single transmitter-receiver set that provides path-averaged winds normal to the optical path. To resolve the complete horizontal wind vector, an additional transmitter-receiver set must be deployed along an axis perpendicular to the first optical path. If scintillometers are deployed so that their lines of sight form a triangle, the three path-averaged wind components can be used to determine the net horizontal flow into or out of the triangle (divergence).

Scintillometers are small, portable, remote-sensing instruments that can operate on battery, solar, or commercial power. They can be deployed in locations where fixed-point sensors are impractical, or where path-averaged winds are desired. They are also useful for rough terrain and cross-valley wind measurements or for monitoring runway crosswinds. Scintillometers are insensitive to acoustic and electromagnetic noise but can be attenuated by smokes or obscurants drifting across the optical path. They cannot be operated under conditions when direct sunlight impinges on the transmitter or receiver optics. Scintillometers can operate in precipitation as long as the optical path is not obscured.

Finite-Aperture Scintillometers. The finite aperture optical scintillometers currently in use include the NOAA Wave Propagation Laboratory (WPL) Model II described by Ochs et al. (1980) and the WPL Model IV (Ochs and Cartwright, 1980), modified to Model IV-L by the Lockheed Engineering and Management Services Company, Inc. (LEMSCO, 1984). The WPL Model II consists of a single-barrel transmitter and receiver with 15-cm optics for

measurement of C_N^2 along the optical path. The WPL Model IV has a double-barrel receiver for simultaneous space-averaged wind and C_N^2 measurements. The WPL Model IV-L is essentially a Model IV manufactured with sealed optics and electronics hardened for field use.

The WPL Models II and IV optics with a $0.94 \mu\text{m}$ LED provide an operating range for C_N^2 between 10^{-12} and $10^{-16} \text{ m}^{-2/3}$. The system saturates if operated during high turbulence conditions ($\sim 10^{-12} \text{ m}^{-2/3}$) over an optical path in excess of 900 m. Saturation produces erroneous readings that appear as a flattening of the C_N^2 profile. The transmitter and receiver can operate in open air from stable tripods, or they can operate through windows in instrument shelters. A stable platform is essential for maintaining system pointing and to minimize vibrations that may contaminate C_N^2 data. Careful alignment onto the main beam is needed (an oscilloscope is recommended for locating peak signal strength); pointing errors are the main cause of scintillometer signal degradation. The background behind the transmitter should also be stationary. Excessive movement of leaves or vehicles can contaminate the signal. The models II and IV scintillometers have a single broad weighting function centered near the middle of the optical path, which means that wind and C_N^2 measurements are weighted towards mid-path conditions. The theoretical weighting function is presented in figure 3-2(a).

Spatially-Averaged Filter Scintillometers. Spatial filtering, based on a technique proposed by Lee (1974), is able to provide relatively sharp path resolution for measurements of wind and C_N^2 at multiple positions along an optical path. Paired zero mean filters in the transmitter and receiver, consisting of alternate dark and clear stripes of selected widths, convert optical turbulence from refractive fields translating across an optical path to sinusoidal perturbations on the receiver's focal plane. According to Lee's theory, a spatial filter of a specific wavelength allows only one wave number at a specific optical path position to generate illumination intensity variance at the receiver. Therefore, the transport by wind of the correct size turbulence elements across an optical path is measured as a set of temporal frequencies at the receiver. With multiple source and receiver filter sizes, and assuming that Taylor's "frozen turbulence" hypothesis is not seriously violated, cross-path wind and C_N^2 measurements can be simultaneously made at multiple positions along an optical path.

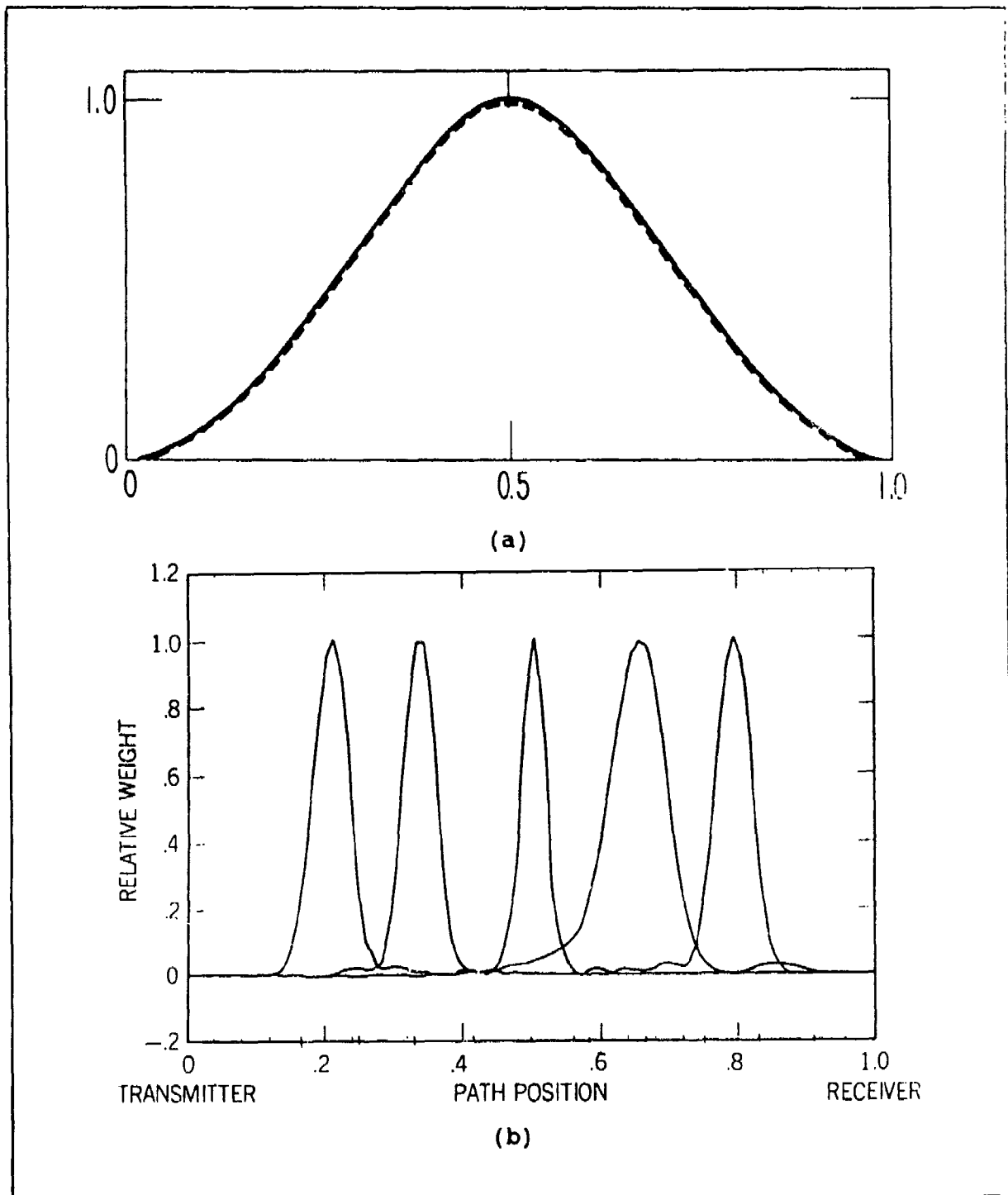


Figure 3-2. Theoretical weighting functions for the (a) WPL Models II and IV finite aperture scintillometers, and (b) the spatially-averaged filter scintillometer.

Spatial-filter sizes are chosen as a compromise between the desire for sharp, well-defined weighting functions that define the instrument's sensitivity to a specific portion of the optical path, susceptibility to saturation effects, and a good signal-to-noise ratio. Path-weighting functions calculated for selected filter-defined wave number combinations used in the spatially-averaged filter scintillometer are shown in figure 3.2(b). The weighting function for the WPL Model II finite aperture scintillometer is shown in figure 3.2(a) for comparison.

Other Remote Sensors and Remote Sensor Combinations

Other remote sensors such as radars and lidars are used for measurements within the planetary boundary layer, although mostly for research purposes. Lidars use backscatter from particulate matter in the atmosphere to obtain range and velocity information. Some lidars are also designed for water-vapor measurements. They offer excellent resolution but are limited in range to 1 km unless very high power and pulse modulation are used. In some situations, the aerosol concentrations are too low to produce a sufficient backscattered signal. Lidars are increasingly used for research on diffusing clouds because of their ability to define cloud dimensions.

Frequency modulated, continuous wave (FM-CW) radars use radio frequency energy backscattered from atmospheric temperature and moisture inhomogeneities to provide high resolution winds as well as temperature and moisture gradient data. With a height range from several hundred to several thousand meters, this equipment can be used to estimate height of the mixed layer.

Radar and acoustic profilers used in combination constitute a radio-acoustic sounding system (RASS) that is used to obtain profiles of winds and temperature. The RASS consists of a vertically directed acoustic transmitter matched for Bragg resonance to a collocated radar array. The vertical propagation of an acoustic pulse is tracked by the radar, and the speed of sound is determined from the radar frequency Doppler shift off the propagating acoustic wavefront. Because the acoustic pulse propagation speed varies as the square root of the virtual temperature, temperature profiles can be estimated by making some assumptions about the distribution of moisture and vertical velocity in the atmosphere. The RASS techniques work with either a radar unit matched to an acoustic sounder or an audio transmitter matched to a radar wind profiler. The vertical temperature structure of the atmosphere is of great interest for air-quality monitoring and diffusion modeling, and RASS temperature profiling techniques are used in Europe and South Africa for these purposes. Surridge (1986) describes the principles and applications of RASS temperature profiling.

The accuracy of RASS temperature profiles is limited by the validity of the assumptions used to estimate temperature from sonic temperature and by the magnitude of the vertical velocity component. The RASS temperature measurement errors are approximately 0.37 percent per degree Celsius of sonic temperature uncertainty, and 0.6 percent per meter per second of vertical wind error. Therefore, substantial errors are possible in the presence of a strong humidity gradient or convection. In addition, horizontal winds deflect the acoustic pulse, and winds in excess of 15 m/s may cause data loss by deflecting the returning acoustic wavefront away from the receiver. In spite of these limitations, RASS profiling can provide information on the evolution of lower tropospheric temperature structure that is otherwise unavailable.

Visibility Meters

Several manufacturers produce instruments which directly measure visibility using forward scatter techniques. The instruments can operate on either commercial or battery power and can be used for either fixed or mobile applications. Since visibility is essential in electro-optical calculations, its measurement at several points is recommended as is frequent calibration. The instruments commonly operate at either 0.904 μm or 0.55 μm . Either is acceptable for most uses.

Transmissometers

These instruments measure the percentage of loss in a beam of energy caused by absorption and scattering by the atmosphere. The instrument must have a source (usually a blackbody oven and/or tungsten halogen lamp) and a downrange receiver. Receivers are chosen to match the spectral interval of interest. Depending on calibration techniques, the measurements can be absolute, relative to clear air, or relative to a clear-air transmittance model calculations. These instruments usually operate over a pathlength of from 0.5 km to 5 km.

CHAPTER 4

PASSIVE REMOTE-SENSING INSTRUMENTS

Lightning threat warning instruments are used to monitor atmospheric electrification and to determine when a lightning hazard is developing. Atmospheric electrification becomes a concern when the surface potential gradient changes from the "fair weather" condition of approximately +100 V/m to -2 kV/m or more, a level where trees and other rounded or pointed objects tend to go into corona discharge. Hasbrouck (1991) suggests that a lightning warning be issued for potential gradients in the ± 1 to ± 1.5 kV/m range, and alarms be issued when the gradient exceeds ± 2 kV/m. Note that these values should be exceeded for 30 s to 1 min prior to issuing a warning or alarm. Figure 4-1 shows the relationship between the recommended alert and danger criteria and the typical evolution of the potential gradient field. Figure 4-1 does not illustrate the "end-of-storm" oscillation, typical of thunderstorms, in which the potential gradient becomes positive, returns to negative, and finally returns to the positive fair weather value. This phenomena is attributed to the combined effects of a diminishing negative charge in the cloud and the presence of a positive space-charge layer. Radioactive probe, corona-current, and electric field mill systems are used to monitor the potential gradient.

Radioactive Probes

A radioactive probe uses a low-level, α -emitting, radioactive source to produce an ionized path between the probe and the volume of air surrounding it with the ions carrying charge to the probe (Chalmers, 1967). A high-impedance electrometer is used to measure the atmospheric potential. The average potential gradient is obtained by dividing the difference in atmospheric potential between two vertically separated points by their separation distance. Because it measures the actual atmospheric potential and is relatively portable, a radioactive probe is useful for field calibration of other lightning threat warning systems. Problems with the radioactive probe stem from the radioactive source and the need to maintain a stable high input impedance. Because the polonium source has a half life of approximately 130 days, it requires measurement compensation as it ages and should be replaced at least annually. Although it is a low level source, reasonable care must be exercised in handling and disposing of the radioactive element. Impedance changes because of resistor aging and the accumulation of dust and other

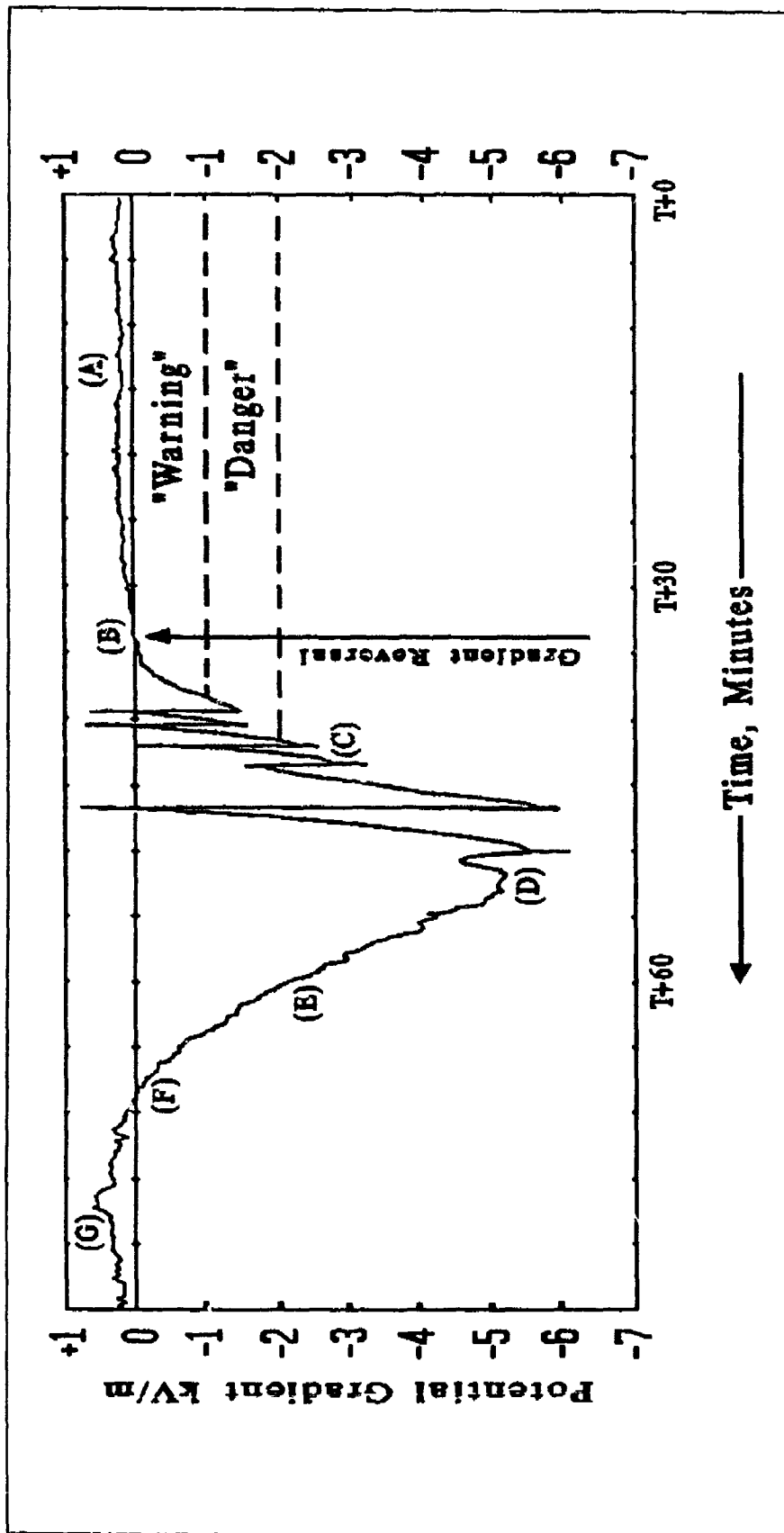


Figure 4-1. Typical evolution of the surface potential gradient during a thunderstorm event. The typical fair-weather field gradient is 100-200 V/m (A). As the storm develops a field polarity reversal occurs (B) and magnitude of the potential gradient increases, exceeding the "warning" and "danger" levels. Lightning-induced spikes occur (C) as the storm evolves, with a maximum value near -5 kV/m (D) for ground-based sensors. The declining phase (E) is characterized by few (if any) lightning events, and the potential gradient again crosses zero (F) and reverts to a fair-weather polarity and intensity (G).

(Source: Airborne Research Associates, Inc.)

particulates on the probe surface also degrade performance. System nonlinearities also occur as a function of temperature, humidity, and high voltages. Markson (1988) describes a negative feedback techniques using a null-sensing circuit that overcomes non-linearity, impedance drift, and insulation leakage problems.

Corona-Current Systems

A conventional corona-current instrument consists of (1) a sharpened points that goes into corona discharge at and above a surface potential gradient of approximately 3 kv/M, and (2) a means for measuring current in the low-microampere range. While useful for measuring the large gradients associated with thunderstorms (for research), this instrument cannot provide pre-first-flash warnings (potential gradients in the 1 to 2 kv/m range).

An instrument known as an active corona-current sensor is currently being evaluated. This instrument measures the magnitude and polarity of the atmospheric electric potential by means of a sharpened point that is elevated from 10 to 20 m above the ground. Applying a high-voltage ac excitation to the corona point keeps it in continuous corona-current discharge. This allows the sensor to measure low values of potential gradient, including those existing in fair weather. The active corona-current sensor is calibrated by comparing its output signal to the actual surface potential gradient measured with radioactive probe.

It should be understood that the true surface potential gradient can be measured only directly at ground level. The radioactive probe and corona-current instruments measure the atmospheric potential (relative to ground) at their respective tips. The surface gradient is then implied by dividing the measured potential by the height of the tip above ground. The values obtained are satisfactory for their intended purposes. Data from the probe and corona-current instruments should be recorded simultaneously (for example, using a dual-channel strip-chart recorder or equivalent) to correlate the data. Recording should be done remotely so that thunderstorm fields can be measured without placing personnel at risk, and the recording system should be lightning protected.

Electric-Field Mills

An electric field mill (EFM) is an electromechanical instrument consisting of a horizontal fixed electrode (stator) made up of several individual conductors and a parallel, segmented, grounded, conductive plate (rotor). (Note that the rotor and stator may be pointed upward or downward.) The rotor is driven at speeds of several thousand rpm and positioned so that it

alternately shields and exposes the stator to the ambient electric field. During exposure intervals, bound charge is induced onto the stator segments by the electric field. When shielded, the stator discharges to Earth through a sensitive current-measuring circuit. Upon re-exposure, charge returns from the Earth via the current sensor and back to the stator. The resulting ac voltage is rectified and filtered, yielding a bipolar dc signal proportional to the potential gradient. When lightning discharges occur, they show up as large amplitude, short duration transients having a polarity opposite to that produced by the storm cell (that is, a positive spike when the cloud-produced gradient is negative). Computer-based analysis of data from a network of EFMs can be used to locate storm-cell charge centers.

The EFMs have several shortcomings. The motor and associated rotating components experience rotational wear. Rotor damage and deterioration are caused by direct contact with hard objects and erosion from wind-borne particles and precipitation. Keeping an EFM in calibration requires routine maintenance to ensure that the rotor segments remain flat and that both the stator and rotor surface are free from the buildup of particulates.

A laboratory method of EFM calibration involves mounting the unit in a fixture consisting of two large-diameter metal plates that are maintained exactly parallel to each other by means of lossy insulators. The plane of the stator is in the plane of lower plate. Large plate surface areas are required to ensure that fringing such as distortion of the uniform field does not occur. A range of dc voltages is applied between the plates (for example, 1 kV across 1 m produces a potential gradients of 1 kV/m), and the EFM electronics are adjusted to provide the desired output.

A field location for an EFM must be carefully chosen. It must be located away from any surrounding tall object by a distance of at least twice the object's height to preclude shielding effects (decreased sensitivity). If an EFM is mounted with its stator elevated above the surface, the resulting field enhancement (increased sensitivity) must be compensated (Atmospheric Research Systems, Inc., 1989). Field calibration can be performed using radioactive probe, located so as not to distort the field near the EFM, to measure the actual surface potential gradient and allows the EFM's in situ response to be determined.

The phenomenon of space charge presents a problem for EFMs. When the potential gradient exceeds about -2 kV/m, grounded-pointed objects on the Earth's surface will begin to go into corona-point discharge. Corona discharge produces a layer of positive ions that masks a surface-mounted EFM from the true magnitude of the cloud-produced field. In addition, an elevated EFM's enhancement compensation will no longer be correct, causing the instrument to essentially become uncalibrated. Even if an

EFM's immediate environment is free from corona-producing pointed objects, it is possible for surface winds to blow space charge in from nearby corona-producing areas. The relatively low mobility of the ions allows space charge to persist for 5 minutes or longer after the cloud-produced field that generated it has decreased in magnitude. Thus, as a storm dies or moves away, the slow-to-dissipate, positive space-charge layer may dominate the electric field, causing the EFM to report a positive-tending potential gradient even though a weakened but potentially hazardous negative charge center may still be present overhead.

The EFMs can also operate well above the Earth if they are elevated by means of sounding rockets, tethered balloons, or aircraft. The airborne field mill system uses EFMs mounted at several positions on an aircraft or other platform to measure electric fields aloft that could adversely affect rocket launches (Kositsky et al., 1991).

Pre-Cloud-to-Ground Lightning Warning and Cloud-to-Ground Lightning Tracking

Potential gradient measurements are useful for identifying point or local area lightning hazards but are not effective for monitoring distant convective or frontal storm systems. A variety of optical, acoustic, and electromagnetic remote sensing instruments are available for detecting intracloud (IC) and cloud-to-ground (C-G) lightning. These instruments are typically operated in multi-sensor arrays situated over a wide area and may be correlated with data from other instrumentation such as weather tracking radar.

Sferics Detectors. A sferics detector or flash counter, tuned to the extremely low-frequency portion of the lightning stroke spectrum, responds to changes in the electrostatic field created by a lightning stroke. Electrostatic field intensity varies inversely with the cube of distance from the source. This rule and the assumption that the received signal was produced by an average amplitude flash, permit a first-order estimate of distance from the flash. While this assumption is poor for any given lightning event, statistical averaging of a number of strokes can provide a reasonable range estimate.

Electro-Optical Sensors. The electro-optical lightning sensor is a handheld instrument that can, when pointed at a cloud, detect IC lightning discharges that are not visible to the eye. This instrument can also be used in an unattended surveillance mode by affixing it to a rigid support and connecting its electrical output to an alarm system. By means of a small, flat-plate antenna and associated electronics, this sensor can also detect the transient electrostatic field component of an IC or C-G discharge.

Locating Intracloud Discharges. A recently developed French system known as SAFIR uses a network of VHF receivers separated by 20 to 100 km and interferometry techniques to determine the azimuth and elevation of pre-lightning electrical discharges and IC lightning. Although SAFIR can locate C-G lightning, it cannot differentiate it IC from lightning. A complete SAFIR system also incorporates EFMs to measure local potential gradients.

Magnetic-Direction Finding. This technique locates C-G lightning using radio-direction-finding techniques. A pair of vertically polarized, orthogonal, cross-loop antennas receive the time-varying magnetic component of a lightning flash. The ratio of voltages induced in the loops is proportional to the tangent of the angle between the plane of the reference antenna and the bearing, or line of position (LOP), to a lightning return stroke (Uman, 1987). A companion flat-plate, electric-field antenna is used to identify flash polarity and to verify that a valid C-G lightning signal has been received. Although single receiver magnetic-direction finding (MDF) systems are in use, the most common configuration incorporates several receiver sites separated by tens to hundreds of kilometers. Lightning location, along with polarity and magnitude information, is recorded and also displayed on a map depicting the area of interest.

The MDF systems are adversely affected by magnetic anomalies located close to the antenna. Nearby power transmission lines and natural or man-made conductors on or beneath the surface distort the magnetic field pattern causing a systematic or site error. Antenna misalignment is also considered to be a source of site error. Where site errors do not vary with time, statistical-analysis techniques can be used to calculate site error correction factors.

Time-of-Arrival. This system receives the very low frequency (VLF) electromagnetic signal from a stroke (IC or C-G) by means of a vertical whip antenna. Typically, four to six receiver sites 200 to 300 km apart are used. A signal is time tagged as it arrives at each receiver, and this tagged signal is transmitted to a central computer for processing. The difference in arrival time at a receiver pair identifies a family of hyperbolas along which the signal originated. Each receiver pair provides a hyperbolic LOP. The intersection of two or more LOPs indicates the location of the stroke (Geitz et al., 1991). Stroke location, lightning type (IC or C-G), polarity, magnitude, and time data are recorded and also displayed on a map.

Accurate timing is maintained by regularly synchronizing each receiver's internal time reference by means of precision timing pulses received from LORAN stations, satellites transmissions, or TV stations. As with any receiver, a time of arrival (TOA)-system antenna must not be shielded by large metallic structures. However, TOA systems do not have any special alignment requirements and are unaffected by magnetic anomalies.

Radiometric Profilers

Radiometric profilers provide vertical profiles of tropospheric temperature and humidity using ground-based, upward-looking, multichannel radiometers operating in the 20- to 70-gigahertz (GHz) frequency range. These radiometers use differential absorption signatures of oxygen, water-vapor, and liquid water to define the atmosphere's temperature and humidity profiles. Oxygen is a well-mixed atmospheric constituent with an absorption coefficient known to a first approximation as a function of altitude. On the other hand, water-vapor and liquid water are highly variable atmospheric constituents. The radiometer receives integrated readings from each of six channels. Complex mathematical inversion techniques have been developed to relate relative signal signatures in each of these channels to the temperature and amount of water-vapor found at different levels in the atmosphere. Statistical techniques are used to match radiances with radiosonde data or other direct measurements to produce smoothed, atmospheric temperature and humidity profiles. Surface temperature and humidity observations provide an absolute reference point for the profiles. Integrated quantities such as total precipitable water are also derived from radiometric profilers. Radiometer data inversion techniques continue to evolve, and radiometric profiling should see widespread applications in the 1990s. Radiometric profilers offer remote, unattended operation to complement wind profiler measurements. Functional precision is only tentatively known but appears comparable to that of radiosonde data within the first 5 or 6 km above the surface. Precision deteriorates progressively at higher elevations.

Plant-Canopy Analyzer

The plant-canopy analyzer provides a non-destructive measurement of leaf-area index, which is a measure of forest-foliage density. Leaf-area index is used to characterize vegetation conditions in dispersion models. The sensor consists of a fisheye lens that focuses a near-hemispherical image onto a photodiode array. The array consists of five concentric rings, each providing view angles of a portion of the canopy or sky. The fraction of diffuse incident radiation passing through the canopy (the gap fraction) is inversely proportion to the foliage density as measured in terms of light received on various parts of the photodiode array. Instrument operating assumptions

include (1) foliage acts as a blackbody with no light transmitted through or reflected from the foliage, (2) foliage elements are small compared to the area of view for each ring, (3) foliage is randomly distributed within each foliage-containing envelope, and (4) foliage is randomly distributed in azimuth.

Real canopies violate these assumptions to varying degrees, and users must compensate for these effects. Techniques for deducing foliage density from gap fraction measurements are described by Perry et al., (1988). The plant-canopy analyzer is best used just before sunrise or after sunset or when there is a thick, uniform cloud cover.

Actinometers

Solar and terrestrial radiation measurements are sometimes used to estimate atmospheric stability for diffusion models. Net radiation, the difference between the incoming (solar and diffuse sky) and outgoing (terrestrial and reflected solar) radiation, defines energy gain or loss near the earth's surface. Net energy gain decreases stability and increases the atmosphere's diffusive power. The converse is true for net energy loss. Instruments which measure solar or terrestrial radiation are called actinometers. The use of actinometers for radiation and sunshine measurements is covered in the WMO Guide (1983).

Actinometers measure the intensity of radiant energy at a surface within certain spectral bands. Intensity of the radiative flux defines the energy per unit time (radiative power) per unit area. An actinometer that measures shortwave radiation (wavelengths of 0.3 to 4.0 micrometers, μm) is called a pyranometer, while an actinometer that measures long-wave radiation (wavelengths of 4 to 50 μm) is called a pyrgeometer. Pyranometers and pyrgeometers measure the exchange of radiation between a horizontal blackened surface and the sky or ground. To resolve the net radiative flux through a surface, sets of pyranometers and pyrgeometers are mounted with one pyranometer-pyrgeometer pair facing up and the other facing down. The net radiation is given by the difference between the incoming and outgoing short- and long-wave radiation. Net radiative flux can also be measured using a net radiometer, or pyrrometer. Special purpose actinometers are available for measurement of ultra-violet radiation, and filters are used to measure specific frequency bands within the solar spectrum. Shadow bands are devices used to block out direct sunlight for measurement of the diffuse sky component of radiation.

Pyranometers. Pyranometers use thermopiles, silicon cells, or bimetallic strips as detectors, while pyrgeometers use thermopiles. A thermopile consists of a series of thermoelectric junctions between two dissimilar metals. A temperature gradient between junctions is generated by placing one set of junctions in

thermal contact with a nonwavelength-selective black surface while isolating the other set. The temperature gradient produces a voltage that is proportional to the temperature difference and hence to the intensity of incident radiation. These actinometers are usually covered with Schott glass domes to minimize contamination and convective heat loss. Silicon photoelectric cells consist of differentially doped semiconductor plates. An electric charge develops when the cells receive radiation, and the electrical resistance changes in proportion to the incident radiant energy. Unlike thermopiles, the performance of these cells is highly dependent on the wavelength of incident radiation. A bimetallic strip consists of fused metals with different thermal expansion coefficients. Sunlight falling on the darkened bimetallic strip causes it to heat and bend with the change of position scaled to provide a measure of the incident radiation. This type of instrument, which is usually mechanically linked with an analog strip chart recorder, provides the least accurate readings. Pyrgeometers are covered with silicon glass to minimize short-wave radiation effects. A limiting factor for accuracy of all of these instruments is the occurrence of temperature gradients and convective currents within the dome. The most accurate actinometers are temperature compensated to minimize sensor thermal effects.

Table 4-1 lists the response times and accuracies of different types of actinometers. Actinometers must be sited where they have unobstructed exposure to the target of interest such as the sky or ground, and their protective covers should be cleaned frequently. Care should be taken to keep an actinometer out of shadows and ensure that it does not receive radiation reflected from nearby structures. The horizon angle should be less than or equal to 5° for good solar exposure. Accuracies on the order of ± 5 percent and a time constant of 30 s or less are sufficient for most radiation measurement applications. Actinometer output is typically 3 to 30 millivolts per gram-calorie per square centimeter per minute ($\text{mV/cal/cm}^2/\text{min}$). Instruments which provide the greatest millivolt output are the most sensitive and accurate. A recorder with good resolution and low-noise level is required for radiation measurements.

Pyranometers should be recalibrated annually at a radiation standards laboratory. Silicon cell pyranometers can be calibrated using a precision spectral pyranometer transfer standard and procedures presented by Aceves-Navarro et al. (1988). Standard error estimates on the order of 20 W m^{-2} can be achieved using this method.

Pyrgeometers. Pyrgeometers are similar to pyranometers except they are designed to operate in the $3\text{-}50 \mu\text{m}$ band.

Pyrheliometers. Pyreheliometers are designed for measurement of direct solar intensity for either total or spectral measurements. The sensor is a thermopile, with a ± 1 percent accuracy over a temperature range of -20 to $+40$ °C, mounted in a pressure-sealed brass tube. The instrument includes azimuth and elevation rotation to maintain track of the solar disk. Typical sensitivity is 8 microvolts per W/m^2 . ASTM-E816 (1984) describes calibration procedures for pyrheliometers and their use as secondary reference standards for field use.

TABLE 4-1. TYPICAL ACTINOMETER RESPONSE

Actinometer Type	Sensor Type	Response Time	Accuracy(%)
Pyranometer	Bimetallic	5 min	± 10
Pyrgeometer	Thermopile	1-5 s	± 2
Pyranometer	Silicon Cell	.01 s	± 5
Pyranometer	Thermopile	1-5 s	± 1
Pyrradiometer	Thermopile	12 s	± 5

CHAPTER 5

AIRBORNE INSTRUMENTS

In general, airborne-meteorological sensors are fixed-point sensors mounted on a moving platform. Airborne sensors are used to extend measurements higher into the atmosphere or over greater horizontal distances than would otherwise be possible. The advantages of using an airborne sensor rather than multiple fixed-point sensors to sample along a measurement path are (1) the effects of differences in instrument calibration and response are eliminated, and (2) the required number of sensors is minimized. Some airborne sensors are mounted on platforms designed to travel with and measure within a cloud or plume.

The limitations of airborne meteorological measurement systems are primarily attributable to the airborne platform. Time on station is limited by airborne platform endurance. An ascending balloon, for example, makes a single pass through the atmosphere. Sensor ventilation rates vary with speed, altitude, and angle of exposure, and the field of view is often limited by platform or structural requirements. Additionally, aircraft-mounted sensors must be sufficiently rugged to withstand mechanical vibration, acceleration forces, and wind forces. Instruments are limited by the tradeoff between robust design and sensitivity. The effects of skin friction heating, flow distortion, and platform heat conduction should be accounted for during analysis of the data. A sensor mounted on a rapidly moving platform such as an aircraft also requires high sampling rates or substantial data smoothing to minimize the effects of undesired platform motions. Finally, time and position data must accompany sensor measurements.

Free Balloons

Free balloons are the most commonly used airborne sensor platforms. Free balloons are released with or without attached instrument packages and are optically or electronically tracked. Although most free balloons are designed to ascend through the atmosphere, one class of free balloon called the tetron is designed to float at a constant level. In either case, it is assumed that the balloon has negligible inertia and travels with the free air flow. Because of shape deformation and vortex shedding, rising free balloons tend to produce undesired oscillations as they ascend. Instrument packages attached below a free balloon (the balloon train) increase inertia and can cause pendulum motions as the package swings below the balloon. The effect of these extraneous motions can be minimized by data averaging and using large separation distances between the

balloon and train. Some balloons are manufactured with a rigid, dimpled surface to minimize oscillations. Fichtl (1972) presents an analysis of the dynamic response of a balloon in the atmosphere which includes drag, lift, virtual-mass effects, and buoyancy effects.

Pilot Balloons. Pilot balloons (PIBALS) are the simplest of the free balloons. They come in 10-, 30-, and 100-g sizes (based on balloon weight) and a variety of colors to aid optical tracking. Ten-gram balloons are used mainly for cloud-height estimates, where time of disappearance into clouds and an assumed ascent rate provide a measure of cloud-base height. The PIBALS of the 30- and 100-g sizes have ascent rates that are large in comparison with atmospheric vertical motions and are, therefore, useful for estimating horizontal wind data. Optical tracking with a theodolite for azimuth and elevation plus an estimated ascent rate permit a balloon's position to be estimated at given time intervals. A vertical profile of wind speed and direction is then calculated using the theodolite-derived azimuth and elevation angles and the assumed ascent rate. Optically tracked single theodolite observations are the least accurate means of measuring upper level winds. Double-theodolite PIBAL tracking increases precision by directly determining the three dimensional position at the expense of coordinated tracking by two theodolite crews.

The PIBAL wind profiles are the easiest and least expensive to obtain but have several limitations. Measurement precision is limited by geometry. At low-elevation angles, small angular changes result in large changes in the estimated winds. Also, inaccurate readings occur as a PIBAL passes through shear zones. Tracking is lost if the balloon drifts into the proximity of the sun or enters a cloud. The PIBAL winds become unrepresentative if the balloon encounters rain or strong updrafts or downdrafts. Measurement representativeness can be increased by averaging winds from sequential PIBAL releases. Single-theodolite PIBAL precision is on the order of 2 to 4 m/s when the atmosphere exhibits negligible vertical velocity. Pilot balloons are sometimes fitted with a radar reflector (typically strips of aluminum foil) to produce a radar ball (RABAL) for radar tracking. Radar tracking provides range-to-target information and eliminates the need to use estimated balloon rise rates. The RABAL accuracy is a function of radar settings and balloon elevation angle.

Jimspheres. Jimspheres are large, rigid, dimpled balloons with a radar reflective surface covering. They are designed to minimize extraneous balloon motions caused by vortex shedding and require no additional reflector attachments. Radar-tracked Jimsphere precision and resolution vary as a function of radar condition, settings, and operating procedures. Root-mean-square errors of 0.5 m/s are reported by Susko and Vaughan (1968) for

elevation angles above 12.9 degrees and target ranges of 80 km or less. A Jimsphere system provides the most precise wind measurement capability currently available but is also the most costly and demanding of range resources. Jimspheres are typically used to obtain detailed wind profile information from near the surface to 30 km.

Radiosondes. The most frequently used free-balloon system is the radiosonde. A radiosonde is a small battery-powered instrument package attached beneath a balloon. The instrument package typically contains a thermistor for temperature measurements, a hygistor for humidity measurements, and a pressure sensor. As the balloon ascends, the pressure cell expands, moving an arm across contacts on a commutator bar or a capacitive pressure sensor. The temperature and humidity or other sensors are time commuted; the commutator switches between temperature, humidity, and reference contacts at predetermined pressure levels. In some systems, pressure is measured capacitively or in a bridge. The battery-powered transmitter sends temperature, humidity, and contact (or pressure) information from the balloon-borne package to the radiosonde ground station. Wind information is obtained either by ground station radio direction finder (RDF) tracking, or by resolving transmitter position from Loran or Omega navigational aid (NAVAID) station timing signals. The functional precision reported by Hoehne (1980) is 3 m/s for older RDF systems but has improved to 1 m/s or better with use of a Loran NAVAJD system. Pratt (1985) estimates temperature errors of 1 °C or less and that relative humidity thermal lag and hysteresis create an uncertainty near 20 percent for the sondes used by the National Weather Service.

Federal agencies operate an array of radiosonde stations across the country. Radiosonde flights are routinely made at 0000 and 1200 Universal Coordinated Time (UTC) to provide comprehensive upper-air information for weather analysis and numerical model input. Radiosondes are designed primarily to obtain wind and thermodynamic profiles to altitudes near 30 km. Although resolution in the planetary boundary layer often is poor, radiosonde data are sometimes the only data available for estimating the height of the mixing layer and mean mixing-layer winds. General radiosonde measurement techniques, sources of error, and calibration procedures are described in the WMO Guide (1983).

Loran Systems. Wind errors for the cross-chain Loran sounding system vary with Loran station geometry. Geometry-induced wind error estimates for the worldwide Loran Network vary from 0.5 m/s or less in regions with good station geometry (including most of North America) to 20 m/s or more over many equatorial regions and areas remote from existing chains (Passi and Morel, 1987).

Omega Systems. Wind errors for Omega-based wind sounding systems also vary with Omega station geometry. The Omega chain is worldwide, whereas Loran chains are regional. However, because Omega station separation is large, geometry-induced measurement uncertainties are on the order of 4 m/s.

Radio Direction-Finding Systems. A radio direction finding (RDF) tracking system consists of a ground-based antenna telemetry receiver and recorder. A radiosonde's azimuth and elevation are obtained from the antenna's track of a frequency-modulated signal from the ascending radiosonde, and height is determined from pressure, temperature, and humidity measurements through solution of the hypsometric equation. Principal sources of error include the effects of thermal lag and solar radiation on the radiosonde's rod thermistor and baseline calibration errors. These temperature and pressure errors introduce errors into hypsometric equation solutions. Additionally, the hypsometric equation is based on the hydrostatic assumption that the atmosphere is in static equilibrium with the net pressure force balancing gravity. This assumption is violated in baroclinic conditions or convection. Position tracking errors arise because of uncertainties in azimuth and elevation angle measurements, which vary with the sensitivity and resolution of the tracking station. Tracking accuracy is a function of the condition of the equipment, beam width, operator skill, and elevation angle of the radiosonde. Angular resolution decreases and ground clutter effects increase at low elevation angles. The RDF measurement techniques, sources of error, and measurement precision are described by Nestler (1983), who reports typical root-mean-square errors of 0.6 °C in temperature and 24 m in geopotential height. Temperature pressure and height errors tend to increase linearly with height for RDF systems (Hoehne, 1980).

Tethered Balloons and Kites

Tethered balloons and kites are used as platforms to measure vertical profiles of wind, temperature, and humidity to heights of up to several km. The utility of tethered devices is constrained by payload weight and wind-speed limitations, but they have the advantage of being able to loiter in position or move vertically under operator control. For this reason, they are sometimes used to verify the performance of remote wind profilers (see Baxter, 1991). Tethered balloon operators report a loss of control when the balloon is exposed to winds in excess of 8 to 12 m/s. Because tethered systems move in response to wind and turbulence, their suitability for flux and turbulence measurements is questionable. Tethered systems have neither the stability advantage of fixed platforms nor the range advantage of aircraft but offer a relatively inexpensive way to obtain vertical wind, temperature, and humidity profiles when weather conditions permit.

Rocketsondes and Mini-Rocketsondes

Most balloon-borne sensors are limited to altitudes of approximately 30 km. Above these altitudes, rocketsondes must be used for wind and thermodynamic profiles. A rocket carries a package containing a datasonde, telemetry system, and aluminized parachute to approximately 80 km, where the package ejects. Temperature data from the datasonde's bead thermistor are transmitted to a ground-based receiver, and radar track of the parachute provides wind and positional data. Pressure and density are then calculated with the aid of a conjunctive radiosonde (corawinsonde) with a "tie-on" point at 20-25 km. One system (PWN 12A Robin) carries an aluminized sphere to apogee at approximately 112 km, where the sphere inflates and begins its descent. Radar track provides wind and density; pressure is derived using the hypsometric equation and thermodynamic data from the corawinsonde. Extraneous heat sources, aerodynamic heating, and radiation strongly influence temperature measurements at high altitudes. Temperature measurements above 70 km are not used, and datasonde temperatures are usually rejected if the temperature at the tie-on point deviates by more than 1.5 °C from the temperature measured by the radiosonde thermistor. Nestler (1983) describes rocketsondes, their error sources, and measurement precision.

Boundary-layer wind and thermodynamic profiles can be measured with a payload carried by a small rocket to heights of 1 to 4 km. Fabricated from paper and plastic, these rockets can be launched without the need for special range access or launch control. The payload, ejected at apogee, provides high (5-m) spatial resolution pressure, temperature, and humidity data as it descends. Mini-rocketsondes are used to provide data for refractive index and inversion height computation.

Dropsondes

A dropsonde is a non-retrievable meteorological instrument deployed from an aircraft. It is released at aircraft altitude and descends to the earth's surface with the aid of a parachute. Dropsondes contain pressure, temperature, and humidity sensors and provide wind speed and direction data. The observed meteorological and positional data signals are modulated onto a carrier signal that is transmitted to the aircraft for processing. The dropsonde's end products are vertical profiles of temperature, humidity, and wind. Dropsondes are ideally suited for deployment over remote land or ocean areas where conventional methods of gathering meteorological data are unavailable.

Early dropsondes provided pressure, temperature, and humidity data only. In the early 1970s, the National Center for Atmospheric Research (NCAR) integrated a navigational receiver into the dropsonde to measure wind data. Since that time, dropsondes

have been used for operational and research purposes. The U.S. Navy, Air Force, and National Oceanic and Atmospheric Administration (NOAA) aircraft have routinely deployed dropsondes during weather reconnaissance flights through tropical and extratropical cyclones. Dropsondes were widely used in the early 1970s in the Global Atmospheric Research Program (GARP), in the mid 1970s in the GARP Atlantic Tropical Experiment (GATE), in the late 1970s in the Global Weather Experiment (GWE), and in the late 1980s in the Experiment for Rapidly Intensifying Cyclones in the Atlantic (ERICA) project. See Julian (1982) for a description of the drop-windsonde system used on the GWE.

The NCAR has been a primary developer of dropsonde technology in the United States since the early 1970s. The current dropsonde under development at NCAR is a lightweight Omega digital dropsonde designed to operate with the U.S. Air Force's Improved Weather Reconnaissance System (IWRS). Future dropsonde enhancements will include the addition of a Global Positioning System (GPS) receiver. This advance will improve the accuracy of derived wind measurements and provide the capability to gather dropsonde height data without a pressure sensor. As technology matures, the ability to place GPS receiver circuitry on a computer chip is anticipated to keep the cost of GPS dropsondes reasonable.

Aircraft-Sensor Platforms

An aircraft sensor platform offers the advantages of mobility and range. Aircraft instrumentation can be as simple as a single thermocouple mounted on a fixed-wing aircraft, helicopter, or drone to a multi-engine aircraft with sensors designed for cloud liquid water content, temperature and moisture fluxes, and turbulence measurements. Specialized instrumentation used on aircraft include air-motion sensors and gust probes. Larger aircraft may carry lidars, radiometers, and electric-field mills. Added aircraft platform advantages include information obtained from a pilot's visual observations, and the pilot's ability to position sensors in the area of interest. Also, aircraft can be equipped with telemetry to relay measurements and video of cloud scenes to ground-based observers. Aircraft sampling is especially useful over water surfaces where the cost of maintaining fixed platforms can be prohibitive. Aircraft measurement applications are described in Lenschow (1986).

Instruments mounted on aircraft require specialized housings to minimize vibration, platform motion, and dynamic heating effects. Velocity, temperature, and humidity sensor readings require adjustments for these effects. Safety certification is required for any airframe configuration changes associated with the installation of instruments or probes outside the aircraft. Lenschow (1986) describes procedures used to isolate aircraft motions and to perform in-flight instrument calibrations.

CHAPTER 6

SAMPLING AND QUALITY CONTROL

Sampling and Averaging Time

Meteorological processes form a continuum in space and time with short-term variations superimposed on long-term trends, whereas meteorological time series measurements are limited to finite space and time scales by the sampling rate and averaging time or length of record. Sampling rate and averaging time constitute low-pass and high-pass filters on data sets. All measurements of frequency higher than the data sampling rate are removed from the data set as are the low-frequency trends of duration greater than the data averaging time. Most meteorological data are presented as statistical quantities such as means and standard deviations or variances. Because the choice of sampling rate and averaging time can significantly affect these statistics, the selection of appropriate sampling rates and averaging times is a major concern. A detailed discussion of the effects of sampling rates and averaging times on turbulence measurements is provided by Pasquill (1974) and Panofsky and Dutton (1984). Spatial averaging because of the length of an instrument's measurement path is described by Silverman (1968). These effects are briefly discussed below.

If each measurement of a meteorological variable is assumed to vary randomly about the true mean value, the true mean and standard deviation about the mean can be determined only by sampling the parameter an infinite number of times. Obviously, an infinite number of samples, which corresponds to an infinite averaging time, is impossible. Thus, a finite averaging time must lead to uncertainties in the statistics. In general, the percent uncertainties in the measured mean and, to a lesser extent, the measured standard deviation decrease relatively quickly with increasing averaging time. A 60-minute averaging time usually is about the longest practical wind and turbulence (wind fluctuation) measurement time in the surface boundary layer because the effects of the planetary diurnal cycle become significant as averaging times increase. Sampling over a period of several minutes is usually sufficient for a statistically stable mean wind speed, temperature, or humidity measurement, although longer averaging times are needed to obtain representative measurements during convectively unstable conditions. Standard deviations require a larger sample size, usually on the order of 15 minutes. Relative estimates of higher moments and spectrum analyses may require sampling over periods on the order of 60 minutes. Typically, an averaging time of 15 to 30 minutes for wind and turbulence measurements is a good compromise for most

applications. Convective instability presents a special case where the dominant scales of turbulent motions must be considered to define an adequate averaging time. Meteorological parameters with less variability than the wind (for example, pressure) usually can be determined with a reasonable degree of accuracy over shorter averaging times.

Once an averaging time is established, it is necessary to consider the desired sampling rate. The sampling rate and averaging time define the number of samples. The selected sampling rate usually is a compromise between the desired accuracy and the cost of data acquisition, processing, and storage. Increasing the sampling rate increases the number of samples and, thereby, decreases the level of uncertainty in the data. Unless measurements are to be made close to the ground (4 m AGL or below) or within a forest canopy, a 1-Hz sampling rate is adequate for most diffusion model wind and turbulence profile inputs. Near the surface or within a forest canopy, turbulence scales are smaller and sampling at a rate of 10 Hz is recommended. The 10-Hz rate is also recommended when measurements are made for flux computations within the constant-flux surface boundary layer. The selected sampling rate should be consistent with an instrument's response characteristics or range resolution.

The sampling rate requirement is an important consideration for selecting instrumentation. The simple $t=x/u$ relationship between spatial averaging distance x , wind speed u , and time t can be used to determine an appropriate sampling rate. Little additional information is gained by sampling at a rate greater than that defined by x/u . Intercomparison tests of mechanical anemometers and vanes with sonic anemometers (Finkelstein et al., 1986) have shown that the frequency response of the mechanical wind instruments falls off at frequencies between 0.1 and 1 Hz. Consequently, mechanical instruments are not adequate for measurement of turbulence scales much below 10 m. Sonic and hot-wire anemometers normally can be used at higher sampling rates. A sonic anemometer begins to lose spatial resolution because of line averaging effects at approximately 2π times the acoustic path length (Kaimal et al., 1968). It is adequate for measurement of turbulence scales in excess of 1 meter. Finer scale turbulence measurements can be obtained using hot-wire anemometers. For mean temperature and humidity readings, instruments with a slow response time (0.1 to 0.01 Hz) are adequate. Temperature or humidity flux measurements should be made with instruments capable of 10 Hz response.

Site Influences

Proper exposure of meteorological equipment is needed to obtain representative data. Measurements should be representative of test site conditions. Wind velocity near the surface changes significantly with height and is greatly affected by irregularities in the ground or by obstacles such as trees or buildings. Likewise, local heat and moisture sources influence temperature, humidity, and gradient measurements. Actinometers must also be located where they are not inadvertently shadowed or subjected to wide variations in temperature.

Typical exposure for wind instruments is 10 m above ground level, although instruments spaced logarithmically in height (for example, measurement heights of 2, 4, 8, and 16 m) often are used to determine profiles and gradients. Mean temperature and humidity are usually measured at the 1.5-m level. These measurement heights are appropriate for open, flat terrain which includes no obstructions within 300 m of the instruments. As a rule of thumb, wind measurements should be made 10 m above the average obstruction height. For example, in the vicinity of small buildings or trees up to 6 m in height, wind instrument exposure height should be at 16 m. Measurements are likely to be adversely affected by eddies generated by obstructions 12 m or more in height. Such large obstacles reduce average wind speeds and cause persistent turbulent eddies. Mechanical sonic anemometer and wind measurements are not recommended at heights of less than 2 m AGL. Hot wire/hot film anemometers are more suitable for velocity measurements close to the ground or in confined areas.

Site selection for wind and turbulence measurements is particularly crucial when large roughness elements are present. Effects of tree lines on wind velocity profiles are discussed by Nord (1991). Large terrain obstacles can generate lee-side eddies which persist. These effects are particularly important for dispersion modeling applications. If a dispersing cloud is affected by these eddies, monitoring instrumentation should be sited to measure these effects. Conversely, if the cloud is not affected by these eddies, instrumentation should be sited to avoid them.

The instrument tower and support structure can also adversely influence wind and turbulence measurements. To minimize structural influences, instruments should be mounted on a boom extending from the tower by at least 1.5 times the tower width. Site surveys and audits should be performed to document instrument performance and exposure conditions. Site and instrument performance audits are described in the Quality Assurance Handbook (1989).

Quality Control

Quality control in meteorological measurements should consist of a combination of automated reasonableness checks during data acquisition and subsequent manual review of the data with editing as required. The initial, automated quality control check should occur as the data enter the data collection system. This first quality control check should include a format check for proper date, time, and sensor identification sequence. The next step in the automated quality control check should flag data received outside of the sensor's output range. For example, wind speed, relative humidity, and precipitation cannot be less than zero or exceed the maximum design output of the sensor. A sensor should also be flagged if wind, temperature, or humidity readings remain invariant for several hours. Once data have passed this initial screening, data should be checked for reasonableness and internal consistency. Some reasonableness and consistency criteria are presented in table 6-1. A comprehensive quality control program for use with a network of mesometeorological towers is presented by Wade (1987). A comprehensive quality assurance program, which begins with management-defined quality goals, is presented in the Quality Assurance Handbook (1989). Several commercial companies are equipped to perform site audits and design quality control programs for meteorological applications. Advertisements for these services are often found in the American Meteorological Society Bulletin.

Data points that successfully pass through the checks in table 6-1 can be formed into averages and variances. Higher moments, the skewness and kurtosis, may also prove useful, although many data points and considerable computation time are required for these computations. Manual review of means, standard deviations, ranges, and higher-order moments can be useful at this stage of the quality control process. Time series plots, trend analysis, and outlier identification are useful at this time.

There is no perfect filter or quality-control technique. Some good data are always lost, and some bad data always pass through any quality-control scheme. Data-evaluation criteria should be a function of data applications with careful consideration of the consequences of valid data loss versus erroneous data inclusion. Also, it generally is preferable to flag a dubious data point rather than delete it, because the dubious value itself can provide some clues about the problem with an instrument. Programming can be used to prevent flagged data from being used in computations. An effective flagging technique that requires only a single pass through a data set is a running-mean sample filter. This filter consists of a data point sample collected from the data set over 10 seconds or some other appropriate period. Each data point is compared with the mean and

TABLE 6-1. REASONABLENESS AND CONSISTENCY
CRITERIA FOR METEOROLOGICAL DATA

1. Persistence or repetition of singular values, particularly those associated with zero or full-scale voltage readings.
2. Consistency between successive readings, perhaps including a data point comparison against a running mean average of previous data points.
3. Comparison against expected seasonal variations such as temperature range.
4. Comparison of sensor output with the output obtained 24 hours previously, based on expected day-to-day variations.
5. Intercomparison of wind speeds, wind directions, or temperatures from sensors located at different levels on the same meteorological tower.
6. Intercomparison of sensor output from one location with a similar sensor output from a second location.
7. Intercomparison of temperature and dew point with the criterion that dew point cannot exceed temperature.

range of this sample, and is either accepted or flagged based on user-defined limits. When a new data point is found to be within limits and added to the filter, the last data point in the filter is dropped. The filter progresses forward in time through the data set by adding and dropping points. A running-mean filter can work well for data that are continuous and slowly changing but is inappropriate for discontinuous data such as rainfall rate. If judiciously applied, this type of filter can remove noise while preserving the high-frequency signal component of time-series data.

When sufficient computational capacity is available, sophisticated data analysis and quality-control tools can be employed. Because the spectra of time-series data are very sensitive to errors, spectrum analysis is an excellent data quality-control tool. Power spectrum and cross-spectrum analysis involves the partitioning of energy by frequency, which shows the relative contributions of frequency scales to the total variance in the data. Abnormal instrument performance appears as unusual spikes or dips in the power spectrum. However, spectrum analysis

requires a considerable computational investment. Advances in computer technology increase the availability of spectrum analysis as a quality-control tool when data quality is a paramount consideration. The covariance between sensor outputs or the time-lagged autocovariance for a single sensor output can also be used for quality control. These procedures are often incorporated in software used to generate data from remote-sensing instrumentation.

Wind-Data Processing

Wind direction and wind speed can be considered separately as independent scalar quantities or in combination as a vector. For applications such as weather forecasting, climatology, and continuous-source diffusion calculations, wind direction and wind speed are often treated separately as scalar quantities. When instantaneous wind vane readings are used to compute scalar averages, the crossover problem at north (0 and 360°) must be avoided. For example, the average wind direction for two instantaneous readings of 355 and 005° is 360° (or 0°), not 180°. This precaution is sufficient for many applications.

The transport of a cloud of diffusing material (instantaneous source) is better described by the mean-wind vector than by the scalar means of wind direction and wind speed. In practice, the vector and scalar averaging computational approaches yield similar results except during periods with highly variable wind directions. Panofsky and Brier (1965) suggest using the ratio of scalar to vector wind speeds as a measure of persistence. Because the vector mean wind speed is less than the scalar mean wind speed during variable wind periods, these two computational procedures can yield significant differences in the dosage (instantaneous source) and concentration (continuous source) predictions when used in Gaussian diffusion models.

Vector mean wind speeds and directions can be calculated by converting the instantaneous wind-speed (S_i) and wind-direction (θ_i) observations to east-west (E_i) and north-south (N_i) wind components

$$E_i = S_i \sin \theta_i \quad (6-1)$$

$$N_i = S_i \cos \theta_i \quad (6-2)$$

The wind direction θ_i in equations (6-1) and (6-2) is defined according to the meteorological convention (that is, measured clockwise from north). This is the direction from which the wind is blowing. The mean east-west and north-south wind components are given by

$$E = \frac{1}{m} \sum_{i=1}^m E_i \quad (6-3)$$

$$N = \frac{1}{m} \sum_{i=1}^m N_i \quad (6-4)$$

where m is the number of instantaneous observations. The vector mean wind speed \bar{u} and wind direction θ are then given by

$$\bar{u} = [E^2 + N^2]^{1/2} \quad (6-5)$$

$$\theta' = \arctan (N/E) \quad (6-6)$$

$$\theta = \begin{cases} 90 - \theta', & E < 0 \\ 270 - \theta', & E > 0 \end{cases} \quad (6-7)$$

(Note that the E wind component is positive for a wind from the west and the S component is positive for a wind from the south.) For a sample of wind angles that are more-or-less Gaussian in distribution, a computationally efficient wind azimuth angle standard deviation is given by

$$\sigma_A = \arcsin [(1-B^2)^{1/2}] \quad (6-8)$$

where

$$B^2 = \left(\frac{1}{m} \sum_{i=1}^m \sin \theta_i \right)^2 + \left(\frac{1}{m} \sum_{i=1}^m \cos \theta_i \right)^2 \quad (6-9)$$

Intercomparison Testing

Performance verification of meteorological instrumentation, particularly remote-sensor systems, ultimately requires field-intercomparison tests. Intercomparison testing can be accomplished in two ways: (1) compare the output of the tested instrument against an accepted transfer standard, or (2) compare estimates of variances obtained from redundant measurements made

by several instruments. Performance verification for meteorological instruments is difficult because meteorological variables are continuously changing in space and time, and it is virtually impossible to measure exactly the same phenomenon with two or more instruments.

Transfer-Standard Method. The transfer-standard method is a means of evaluating the performance of an instrument through intercomparison with a reference instrument. Concurrent measurements are made and performance of the test instrument is defined by the degree of departure of its measurements from the reference instrument's measurements. The transfer-standard method uses bias, comparability, precision, and normalized precision as figures of merit (Hoehne, 1971). Bias is the average difference between measurements of the tested and reference instrument, while comparability is the root-mean-square difference. Precision is the standard deviation of these differences, and normalized precision expresses precision as a percentage of the standard deviation of the variable measured by the reference instrument. These figures of merit are recommended by ASTM-D4430, *"Standard Practice for Determining the Operational Comparability of Meteorological Measurements."*

The transfer-standard intercomparison method is limited by a shortage of instruments that can be relied on to produce acceptable "standard" measurements under field conditions. Virtually every instrument has deficiencies that must be accounted for, and the merits of using any particular instrument are open to debate. For example, Finkelstein et al. (1986) used a sonic anemometer as a transfer standard for intercomparison tests of in-situ wind instrumentation. The Finkelstein et al. conclusions were challenged by Lockhart (1989) who prefers to use a different instrument as a transfer standard.

Variance-Estimates Method. This method, first presented by Grubbs (1948) with subsequent development by Thompson (1963) and Grubbs (1973), involves the separation of concurrent measurements by several instruments into estimates of standard errors of measurement and an estimate of the population variance of the measured variable. For three instruments, these estimates are obtained using variances of differences in readings from instruments 1 and 2, 1 and 3, and 2 and 3. The principal figure of merit is an estimate of each instrument's relative precision, which is the ratio of the estimated population variance to the instrument's estimated standard error of measurement. Relative precision of 10 or greater indicates precise measurement (Thompson, 1963), while a relative precision of 3 or greater is generally adequate for meteorological applications (Biltoft, 1991).

The variance-estimates method relies on a number of assumptions. It is applicable only if the data obtained represent independent realizations of the same process measured by each instrument and include no systematic differences and no correlated-measurement errors. These assumptions are violated to some degree during field-test conditions, but the procedure is applicable if unwanted correlations are small. Biltoft (1991) provides an example of sodar intercomparisons using this procedure.

Grubbs (1973) suggests t-tests to determine the statistical significance of inter-instrument differences. As with all statistical tests of this type, an underlying assumption is that the sample data are uncorrelated. Meteorological data collected sequentially in time are invariably correlated to varying degrees. A measure of persistence or correlation for meteorological data is

$$R_a = (2\sigma/\sigma_d) - 1 \quad (6-10)$$

where R_a is a persistence factor defined by the ratio of the standard deviation of measurements within a data set (σ) to the standard deviation of differences from one observation to the next within that data set (σ_d). An estimate of independent sample size is obtained by dividing the data set sample size by $R_a + 1$. This adjusted sample size can then be used with t-tests to determine the statistical significance of inter-instrument differences.

GLOSSARY OF TERMS

Absolute Humidity: The water-vapor concentration in the air. It is defined as the mass of vapor per unit volume of air. The usual units for absolute humidity are grams per cubic meter (g/m^3).

Absorptance: The ratio of absorbed to incident radiative flux.

Acceptance Angle: The angular distance, centered on a sonic anemometer/thermometer array axis of symmetry, over which the following conditions are met: (a) velocity components are unambiguously defined, (b) flow across the transducers is not obstructed, and (c) transducer shadow corrections adequately compensate for shadow effects.

Accuracy: The absolute uncertainty in a measurement; the degree to which a measurement corresponds to an assumed or accepted "true" value expressed as a bias plus a random uncertainty or precision. In practical applications, an instrument's accuracy is determined by comparison of its measurements to corresponding measurements made by a standard such as a wind tunnel or temperature bath. Measurement system accuracy should consider the accuracy of conversion procedures and transfer functions as well as sensor response. Accuracy is usually stated as a fractional part or percent of the measurement scale.

Acoustic Path Length: The physical distance between transducer transmitter-receiver pairs (transducer separation distance).

Actinometer: A class of instruments used to measure radiant energy intensity which includes pyranometers, pyrgeometers, and pyrhemeliometers.

Adsorption: The adhesion, without penetration or chemical interaction, of a liquid or gas to a solid surface.

Angle of Attack: The angle between flow direction and the orientation of an object immersed in the flow.

ASTM: American Society for Testing and Materials. A standards writing organization with headquarters at 1916 Race Street, Philadelphia, Pennsylvania 19103.

Autocovariance: The covariance of a data point measured at time t with another data point from the same variable at $t \pm Dt$. The autocovariance of a quantity is inversely related to the width of the temporal frequency spectrum of that quantity.

Backscatter: A portion of the electromagnetic energy emitted from a source that is returned toward the source because of scattering by atmospheric turbulence, particulates, or other objects.

Calibration: The process of verifying an instrument or system's operational status, usually accomplished by comparing output or response to a known signal input. Full calibration involves tracing a signal from input through a sensor and all transducers, translators, and electrical circuitry to the recording device and should include a series of measurement points covering the span of measurement.

Cospectrum: The real part of the cross spectrum of two functions.

Cross-Spectrum: The Fourier transform of the cross correlation of two functions.

Covariance: The product of two time-dependent quantities. For quantities $\bar{A}(t)$ and $\bar{B}(t)$ with means of A and B, the covariance is $\langle (A(t) - \bar{A})(B(t) - \bar{B}) \rangle$, where $\langle \rangle$ indicates a user-selected time average.

Damping Ratio: The dimensionless ratio of actual wind vane damping to "critical" damping, where no vane overshoot occurs. Damping ratio is inversely proportional to the ratio of two successive vane oscillations after release from an offset position in a wind tunnel. Choice of a damping ratio represents a compromise between rapid response and vane overshoot.

Dew Point: The temperature at which the air is saturated. For air at temperature T and vapor pressure e, the dew point is obtained by decreasing T without a change in atmospheric pressure until e equals the temperature's saturation vapor pressure.

Distance Constant:

1. For a wind vane offset 10° from its equilibrium position in a wind tunnel, the distance constant is a delay distance, the distance traveled by air flowing past the vane during the time taken for the vane to return to 50 percent of its equilibrium position.

2. For an anemometer, the distance constant is a response distance, the distance traveled by air flowing past the anemometer as it reaches $|1 - 1/e|$, or 63 percent, of its new equilibrium position following a step change. The distance constant related to the time constant by $x = ut$, where x is distance, u is wind speed, and t is time.

Emittance: The ratio of radiant existance of a body to that of a blackbody at a given temperature.

Exitance: The flux per unit area leaving a surface.

Hydrostatic Equilibrium: The state of fluid whose surfaces of constant pressure and constant mass or density coincide and are horizontal throughout. Complete balance exists between the force of gravity and the force of pressure. The relation between the pressure and geometric height is given by the hydrostatic equation. The analysis of atmospheric stability has been developed to a high degree for an atmosphere in hydrostatic equilibrium.

Hypsometric Equation: The hypsometric equation is

$$P(\text{SITE}) = P(\text{STN}) \exp \left[\frac{-0.0341\Delta z}{T_v} \right]$$

where

P(SITE) = pressure at the site

P(STN) = pressure at the weather station

Δz = difference in meters between the site elevation and the weather station elevation

T_v = mean virtual temperature in degrees Kelvin (K) for the layer Δz

Illuminance: The total luminous flux received on a unit area of a given real or imaginary surface. Illuminance provides the luminance of a nonluminous surface.

Irradiance: The total radiant flux received on a unit area of a given real or imaginary surface; the flux density of electromagnetic radiation, to be distinguished from illuminance, which refers only to light. Also called radiant flux density, irradiation, specific irradiation.

Luminance: The photometric term corresponding to radiance; specifies the amount of power radiated from an extended body per unit solid angle and per unit projected area of radiating surface; expressed in lumens per steradian per square meter or candles per square meter.

Mixing Ratio: The ratio of the mass of water vapor in a unit volume of air to the mass of dry air in the volume. The usual units are grams per kilogram (g/kg), which must be converted to grams per gram for thermodynamic calculations.

Off-Axis Response: For a rotating anemometer, a ratio of indicated velocity at various angles of attack to indicated wind speed at zero angle of attack, multiplied by the cosine of the angle of attack (ASTM-XXXX).

Overshoot: A measure of the angular excursion past equilibrium that a vane moves when released from an initial 10° displacement off equilibrium. Overshoot is measured as the ratio of two successive deflections of a wind vane as it oscillates about its equilibrium position (ASTM-XXXX).

Precision: The irreducible random response of an instrument to changes in the measured variable. Components of precision include resolution and repeatability.

Range: Span of measurement from the threshold to the maximum measurable value.

Radiance:

1. The radiometric term specifying the amount of power radiated from an extended body per unit solid angle and per unit projected area of radiating surface; expressed in watts per steradian per square meter.

2. In radiometry, a measure of the intrinsic radiant intensity emitted by a radiator in a given direction. It is the irradiance (radiant flux density) produced by radiation from the source upon a unit surface area oriented normal to the line between source and receiver, divided by the solid angle subtended by the source at the receiving surface. It is assumed that the medium between the radiator is perfectly transparent; therefore, radiance is independent of attenuation between source and receiver.

Reflectance: The ratio of the luminous (or radiant) flux reflected from a surface to the total flux (incident illuminance or irradiance) upon that surface. Reflectance varies according to the wavelength and angle of the incident radiation. ($1 > R > 0$).

Refractive Index:

1. Also called index of refraction. A measure of the amount of refraction (a property of a dielectric substance). It is the ratio of the wavelength or phase velocity of an electromagnetic wave in a vacuum to that in a substance. In the atmosphere, it is a function of wavelength, temperature, atmospheric pressure, and water-vapor pressure.

2. The light bending power of an optical material such as glass or plastic; chief identification of optical glass types.

$$n = \frac{\sin i}{\sin r} \quad (\text{Snell's law})$$

where n = refractive index, i = angle of incidence, and r = angle of refraction.

Refractive Index Structure Parameter: The mean-square difference in refractive index (N) over a separation distance (r) between position vectors located at x and $x+r$. Separation distance is typically 10 to 20 cm.

$$C_N^2 = \overline{[n(x) - n(x+r)]^2} / r^{2/3}$$

For a beam of electromagnetic energy propagating through the atmosphere, C_N^2 is a measure of degradation in beam quality because of scintillation. It is the coefficient of the Kolmogoroff 2/3 power structure function law for refractive index as defined by Tatarskii (1961).

Relative Humidity: The ratio of the vapor pressure and the saturation vapor pressure. It often is expressed as a percent.

Repeatability: A measure of how well the instrument is able to gain or shed energy as the instrument is operated from one end of its operating range to the other, described in percent of span. Hysteresis, energy absorption by the instrument that prevents the return to its exact position prior to the energy input, is inversely proportional to repeatability.

Resolution: The least significant digit reading. It defines the smallest variation in the variable input that causes a detectable change in instrument output. It is given as a fractional part of the measurement scale.

Sampling Period: The record length or time interval over which data collection occurs.

Sampling Rate: The rate at which data collection occurs, usually presented in samples per second or Hertz.

Scintillation: The variance in luminance or brightness of a received signal because of turbulence-induced changes in refractive index along an optical path between a light source and a downrange receiver.

Sodar: An active remote sensing instrument that uses sound direction and ranging to obtain wind and turbulence profiles in the atmosphere.

Sonic Anemometer/Thermometer: An instrument consisting of a transducer array containing paired sets of acoustic transmitters and receivers, and microprocessor circuitry to measure intervals of time between transmission and reception of sound pulses. Discussion: The fundamental measurement unit is transit time. With transit time and a known acoustic path length, velocity and speed of sound can be calculated. Instrument accuracy is a function of clock time resolution (described by the increment of velocity resolution), precision of acoustic path length determination, electronic delay, and transducer shadow corrections which describe the interaction of the transducer array with the velocity field in which it is immersed. Instrument output is a series of quasi-instantaneous velocity component readings along each axis and the speed of sound. The speed of sound and velocity components may be used to compute virtual temperature, to describe the mean wind field, or to compute fluxes, variances, and turbulence intensities.

Sonic Temperature: An equivalent temperature closely related to virtual temperature that accounts for the effects of temperature and moisture on acoustic wavefront propagation through the atmosphere. Sonic temperature is defined by absolute temperature T , vapor pressure e , and absolute pressure P (Kaimal and Gaynor, 1991).

$$T_s = T(1 + 0.32 e/P)$$

Specific Humidity: Specific humidity is the ratio of the mass of water-vapor in a unit volume of air to the mass of air in the volume. It differs from mixing ratio only in that it is related to the total mass of dry air plus water-vapor rather than to the mass of dry air alone. The usual units are grams per kilogram (g/kg).

Speed of Sound: Propagation velocity of an adiabatic compression wave through gas,

$$c = (\partial P / \partial \rho)_s^{1/2} = 20.067 [T(1 + 0.32 e/P)]^{1/2}$$

where P is pressure, ρ is density, T is absolute temperature, e is vapor pressure, and subscript s refers to an isentropic (adiabatic) process. Discussion: The velocity of the compression wave defined along each axis of a Cartesian coordinate system is the sum of propagation velocity c plus the motion of the gas along that axis. A nominal value of 340 m/s is used for speed of sound in still air at standard temperature and pressure. For a

speed of sound measurement made by a sonic anemometer/thermometer with an acoustic path length d , the inverse transit time solution is

$$c = \left[\frac{d^2}{4} \left(\frac{1}{t_1} + \frac{1}{t_2} \right)^2 + v_n^2 \right]^{0.5}$$

where v_n is the velocity component normal to the acoustic path, and t_1 and t_2 represent transit times in each direction across d .

Standard Error of the Velocity Estimate: The increment of velocity resolution divided by the square root of the number of samples used to produce each along-axis wind velocity measurement.

Starting Threshold:

1. For a wind vane, it is the lowest wind tunnel velocity at which a vane, released from a position 10° off the vane equilibrium position, moves to within 5° of the equilibrium position (ASTM XXX1).

2. For a rotating anemometer, it is the lowest velocity at which the sensor starts and continues to turn and produces a measurable signal (ASTM D5096).

Taylor's Hypothesis: The small-scale motions by which the turbulent structure of an eddy evolves are much smaller than the mean velocity of the air stream (u) that transports the eddy across a probe or viewing plane. Therefore, for an incremental ytime Δt , the eddy's fine-scale structure appears "frozen" as it translates over an incremental distance Δx defined by $\Delta x = u\Delta t$. Taylor's hypothesis is used to relate the temporal structure measured by fixed sensors to the atmosphere's spatial structure.

Temperature Structure Parameter: The mean-square difference in temperature over a separation distance (r) between position vectors located at x and $x+r$. Separation distances are typically 10 to 20 cm.

$$C_T^2 = [(T(x) - T(x+r))]^2 / r^{2/3}$$

It is a measure of temperature variance.

Thermal Stability Range: A range of temperatures over which the corrected velocity output in a zero-wind chamber remains at or below instrument resolution. Discussion: Thermal stability range defines a range of temperatures over which electronic delay remains constant.

Threshold: The smallest measurable input.

Time Constant: A measure of an instrument's rate of response to a step change in the measured variable. It is the time required for the instrument response to reach $|1-1/e|$ or 63 percent, of the new equilibrium value.

Time Resolution: Resolution of the internal clock of a sonic anemometer/thermometer used to measure time.

Transducer Shadow Correction: The ratio of the "true" along-axis velocity v_{dm} , as measured in a wind tunnel or by another accepted method, to the instrument along-axis wind measurement v_d .

Discussion: This correction compensates for flow-shadowing effects of transducers and their supporting structures. The correction can take the form of an equation or a look-up table.

Transfer Function: An equation that relates the response of an instrument to the true magnitude of the phenomenon that the instrument is designed to measure.

Transit Time: The time interval between transmission and reception of an acoustic wavefront by a transmitter-receiver pair in a sonic anemometer/thermometer array. Discussion: Transit time is determined by path length d , the speed of sound c , the velocity component along the acoustic-propagation path (v_d), and cross-path velocity component (v_n)

$$t = \left[\frac{(c^2 - v_n^2)^{1/2} \pm v_d}{c^2 - (v_d^2 + v_n^2)} \right] d.$$

For each transducer pair, the transit-time difference between acoustic wavefront propagation in one direction (t_1 , computed for $+v_d$) and the other (t_2 , computed for $-v_d$) determines the magnitude of the wind velocity component. The inverse transit time solution for velocity is

$$v_d = \frac{d}{2} \left[\frac{1}{t_1} - \frac{1}{t_2} \right].$$

Vapor Pressure: The total pressure of the atmosphere is the sum of the partial pressures of its constituent gases. Vapor pressure is the partial pressure of water-vapor. The saturation vapor pressure corresponds to the maximum amount of vapor that the atmosphere can hold at a given temperature. Saturation vapor pressure is a function of temperature only. Vapor pressure and saturation vapor pressure usually are expressed in units of millibars (mb).

Virtual Temperature: The virtual temperature (T_v) is the temperature of dry air (T) at the same pressure (P) and with the same density as moist air. It is used in the Ideal Gas Law with the gas constant for dry air to account for density differences between moist and dry air. The normal units are degrees Kelvin (K). Virtual temperature is calculated as a function of T , P , and vapor pressure (e).

$$T_v = T(1 + 0.378 e/p)$$

Virtual temperature and sonic temperature (T_s) are related by

$$T_s = T_v (1 - 0.06 e/p)$$

Virtual temperature can be calculated using tables provided by List (1958).

REFERENCES

- Aceves-Navarro, L. A., K. G. Hubbard, and J. Schmidt, 1988; Group calibration of silicon cell pyranometers for use in an automated network. J. Atmos. Oceanic Tech., 5, 875-879.
- Andreas, E. L., and B. Murphy, 1986: Calibrating cylindrical hot-film anemometer sensors. J. Atmos. Oceanic Technol., 3, 233-298.
- ASTM-D3631, 1990: Method for measuring surface atmospheric pressure, Volume 11.03. American Society for Testing and Materials, Philadelphia, PA.
- ASTM-D4230, 1989: Method of measuring humidity with cooled-surface condensation (Dew-Point) hygrometer, Volume 11.03. American Society for Testing and Materials, Philadelphia, PA.
- ASTM-D4430, 1984: Standard practice for determining the operational comparability of meteorological measurements, Volume 11.03. American Society for Testing and Materials, Philadelphia, PA.
- ASTM-D5096, 1990: Test method for determining the performance of a cup anemometer or propeller anemometer, Volume 11.03. American Society for Testing and Materials, Philadelphia, PA.
- ASTM-E337, 1990: Test method for measuring humidity with a psychrometer (the measurement of wet- and dry-bulb temperatures). (Volume 11.03. American Society for Testing and Materials, Philadelphia, PA.
- ASTM-E816, 1981: Calibration of secondary reference pyrhelimeters for field use, Volume 12.02. American Society for Testing and Materials, Philadelphia, PA.
- ASTM-XXX1 (draft): Standard test method for determining the dynamic performance of a wind vane. American Society for Testing and Materials, Philadelphia, PA.
- ASTM-XXX2 (draft): Standard practice for measuring surface wind and/or temperature by acoustic means. American Society for Testing and Materials, Philadelphia, PA.
- ASTM-XXX3 (draft): Standard test method for determining the performance of a sonic anemometer/thermometer. American Society for Testing and Materials, Philadelphia, PA.

- Atmospheric Research Systems, Inc.: Installation manual for electric field mill (EFM), Revision 1.1, June 1989. Palm Bay, FL.
- Balsley, B. B., 1987: Design considerations for coherent radar systems for probing the troposphere, stratosphere, and mesosphere. 18th conf. on Radar Meteor., Atlanta, GA. Available from the American Meteorological Society.
- Barnston, A. G., 1991: An empirical method of estimating raing-age and radar rainfall measurement bias and resolution. J. Appl. Meteor., 30, 282-296.
- Baxter, R. A., 1991: Aerovironment QA procedures. Aerovironment, Inc., 222 East Huntington Drive, Monrovia, CA 91016.
- Biltoft, C. A., 1987: Development of sonic anemometer software. U.S. Army Dugway Proving Ground, DPG-FR-88-702. AD B120769.
- Biltoft, C. A., 1989: Calibration and quality control for new meteorological instrumentation, Part I. U.S. Army Dugway Proving Ground, DPG-FR-90-705.
- Biltoft, C. A., 1991: An analysis of the 150-m ISIE data. In Preprint Volume Seventh Symposium on Observations and Instrumentation, New Orleans, LA, Amer. Meteor. Soc.
- Brock, F., and C. Nicolaidis, Ed.: Instructor's handbook on meteorological instrumentation. NCAR Technical Note NCAR/TN 237-1A, PB85-105930, June 1984. U.S. Dept of commerce (available through NTIS).
- Brown, E. G., and F. F. Hall, Jr., 1978: Advances in atmospheric acoustics. Reviews of Geophysics and Space Physics, 16, 47-110.
- Buck, A., 1985: The Lyman-alpha absorption hygrometer. 1985 Conf. of the Instrumentation Society of America (ISA), 411-436.
- Chalmers, J. A., 1967: Atmospheric Electricity, 2nd Ed., Pergamon Press, New York, NY, 515 pp.
- Cheney, N. R., and J. A. Businger, 1990: An accurate fast response temperature system using thermocouples. J. Atmos. and Oceanic Tech., 7, 504-516.
- Clifford, S. F., G. R. Ochs, and R. S. Lawrence, 1974: Saturation of optical scintillation by strong turbulence, J. Opt. Soc. Am., 64, 148-154.

- Doviak, R. J., and D. S. Zrnic', 1984: Doppler Radar and Weather Observations, Orlando, Academic Press, 458 pp.
- Fichtl, G. G., 1972: Spherical balloon response to three-dimensional time-dependent flows. National Aeronautics and Space Administration, NASA TMD-6829. Marshall Space Flight Center, AL.
- Finkelstein, P. L., J. C. Kaimal, J. E. Gaynor, M. E. Graves, and T. J. Lockhart, 1986: Comparison of wind monitoring systems. Part I: In situ sensors. J. Atmos. Oceanic Technol., 3, 583-593.
- Finkelstein, P. L., J. C. Kaimal, J. E. Gaynor, M. E. Graves, and T. J. Lockhart, 1986: Comparison of wind monitoring systems. Part II: Doppler sodars. J. Atmos. Oceanic Technol., 3, 594-604.
- Folland, C. K., 1975: Use of the lithium chloride hygrometer (dew cell) to measure dew point. Meteor. Magazine, 104, 52-56.
- Fuchs, M., and C. B. Tanner, 1965: Radiation shields for air temperature thermometers. J. Appl. Meteor., 4, 544-547.
- Garratt, J. R., I. G. Bird, and J. Stevenson, 1986: An electrical-readout, oven-controlled, aneroid barometer for meteorological application. J. Atmos. Oceanic Technol., 3, 605-613.
- Gaynor, J. E., and C. A. Biltoft, 1989: A comparison of two sonic anemometers and fast response thermometers. J. Atmos. Oceanic Technol., 6, 208-214.
- Geitz, W. C., W. H. Highlands, and K. A. Porreco, 1991: LPATS national network (LN)². 7th Int'l. Conf. on Interactive Information and Processing Systems for Meteorology, Oceanography, and Hydrology, Amer. Meteor. Soc., New Orleans, LA.
- Gill, G. C., 1973: The helicoid anemometer. Atmosphere, 11, 145-155.
- Gossard, E. E. and R. G. Strauch, 1983: Radar Observation of Clear Air and Clouds, Elsevier, Amsterdam, 280 pp.
- Grubbs, F. E., 1948: On estimating precision of measuring instruments and product variability. J. Amer. Statistical Assn., 43, 243-264.

- Grubbs, F. E., 1973: Errors of measurement, precision, accuracy, and the statistical comparison of measuring instruments. Technometrics, 15, 53-66.
- Hasbrouck, R., (1991): Lightning-Understanding it and protecting systems from its effects. UCRL-53925. Lawrence Livermore National Laboratory, University of California, Livermore, CA.
- Henning, H., 1971: Zur Messung der Taupunkttemperatur mit dem LiCl - Taupunkthygrometer der Fa. Feutron, Griez, Zeitschrift für Meteorologie, 22, 283-287.
- Hoehne, W. E., 1971: Standardized functional tests. NOAA TM NWST&EL-12, Sterling, VA. U.S. Dept. of Commerce, 23 pp.
- Hoehne, W. E., 1980: Precision of National Weather Service upper air measurements. NOAA Tech. Memo T&ED-16, 12pp.
- Hosom, D. S., G. H. Crescenti, C. L. Winget, S. Weisman, D. P. Doucet, and J. F. Price, 1991: An intelligent chilled mirror humidity instrument. J. Atmos. Oceanic Tech., 8, 585-596.
- Illingworth, A. J., and C. J. Stevens, 1987: An optical disdrometer for the measurement of raindrop size spectra in windy conditions. J. Atmos. Oceanic Tech., 4, 411-421.
- Julian, P. R., 1982: The aircraft dropwindsonde system in the Global Weather Experiment. Bull. Amer. Meteor. Soc., 63, 619-627.
- Kaimal, J. C., J. C. Wyngaard, and D. A. Haugen, 1968: Deriving power spectra from a three-component sonic anemometer. J. Appl. Meteor., 7, 827-837.
- Kaimal, J. C., J. E. Gaynor, H. A. Zimmerman, and G. A. Zimmerman, 1990: Minimizing flow distortion errors in a sonic anemometer. Boundary-Layer Meteor., 53, 103-115.
- Kaimal, J. C., and J. E. Gaynor, 1991: Another look at sonic thermometry. Boundary-Layer Meteor., 56, 401-410.
- Kositsky, J., et al., 1991: Airborne field mill (ABFM) system calibration report. Headquarters, Space Systems Division/CGLR, El Segundo, CA PIIN No. F04701-90-C-0023.
- Kraan, C., and W. A. Oost, 1989: A new way of anemometer calibration and its application to a sonic anemometer. J. Atmos. Oceanic Tech., 6, 516-524.

- Larsen, S. E., J. Hojstrup, and C. W. Fairall, 1986: Mixed and dynamic response of hot wires and cold wires and measurements of turbulence statistics. J. Atmos. Oceanic Technol., 3, 236-247.
- Lawrence, R. S., G. R. Ochs, and S. F. Clifford, 1972: The use of scintillation to measure average wind across a light beam. Appl. Opt., 11, 239-243.
- Lee, R. W., 1974: Remote probing using spatially filtered apertures. J. Opt. Soc Amer., 84, 1295-1303.
- LEMSCO, 1984: Auto-calibrating atmospheric scintillometers model IV-L operation and maintenance manual. Lockheed Engineering and Management Services Company, Inc. (Available from Atmospheric Sciences Laboratory, White Sands Missile Range, NM.)
- Lenschow, D. H., Ed., 1986: Probing the Atmospheric Boundary Layer, Amer. Meteor. Soc., Boston, MA, 269 pp.
- Lewellen, W. S., and R. I. Sykes, 1989: Meteorological data needs for modeling air quality uncertainties. J. Atmos-Oceanic Tech., 6, 759-768.
- Lind, R. J., and W. J. Shaw, 1991: The time-varying calibration of an airborne Lyman- α hygrometer. J. Atmos. Oceanic Tech., 8, 186-190.
- Lindroth, A., 1991: Reduced loss in precipitation measurements due to a new wind shield for raingages. J. Atmos. Oceanic Tech., 8, 444-451.
- List, R. J., 1958: Smithsonian Meteorological Tables. Smithsonian Institution, 527 pp.
- Lockhart, T. J., 1985: Some cup anemometer testing methods. J. Atmos. Oceanic Tech., 2, 680-683.
- Lockhart, T. J., 1989: Accuracy of the collocated transfer standard method for wind instrument auditing. J. Atmos. Oceanic Technol., 6, 715-723.
- Luers, J. K., 1990: Estimating the temperature error of the radiosonde rod thermistor under different environments. J. Atmos. Oceanic Tech., 7, 882-895.
- MacCready, P. B. Jr., 1966: Wind speed measurements in turbulence. J. Appl. Meteor., 5, 219-225.

- Markson, R. J., 1988: High voltage feedback radioactive probe system. Airborne Research Associates Technical Note, Weston, MA.
- Massman, W. J., and K. F. Zeller, 1988: Rapid method for correcting the non-cosine response errors of the Gill propeller anemometer. J. Atmos. Oceanic Tech., 5, 862-869.
- May, P. T., T. Sato, M. Yamamoto, S. Kato, T. Tsuda, and S. Fukao, 1989: Errors in the determination of wind speed by Doppler radar. J. Atmos. Oceanic Tech., 6, 235-242.
- McCaughey, J. G., D. W. Mullins, and M. Publicover, 1987: Comparative performance of two reversing Bowen ratio measurement systems. J. Atmos. Oceanic Tech., 4, 724-730.
- Mori, Y., and Y. Mitsuta, 1987: Some problems in tower wind observations by the propeller-type anemometer. (unpublished report)
- Muller, S. H., and P. J. Beekman, 1987: A test of commercial humidity sensors for use at automatic weather stations. J. Atmos. Oceanic Tech., 4, 731-735.
- Nestler, M. S., 1983: A comparative study of measurements from radiosondes, rocketsondes, and satellites. NASA contractor Report 168343. NASA Goddard Space Flight Center, Wallops Island, VA.
- Nord, M., 1991: Shelter effects of vegetation belts-results of field measurements. Boundary-Layer Meteor., 54, 363-385.
- Ochs, G. R., and W. D. Cartwright, 1980: Optical system model IV for space-averaged wind and C_N^2 measurements. NOAA Technical Memorandum ERL WPL-52.
- Ochs, G. R., W. D. Cartwright, and D. D. Russell, 1980: Optical C_N^2 instrument model II, NOAA Technical Memorandum ERL WPL-51.
- Ochs, G. R., J. J. Wilson, S. Abbott, and R. George, 1988: Crosswind profiler model II, NOAA Technical Memorandum ERL WPL-152.
- Panofsky, H. A., and G. W. Brier, 1965: Some Applications of Statistics to Meteorology, Pennsylvania State University, University Park, PA 224 pp.
- Panofsky, H. A., and J. A. Dutton, 1984: Atmospheric Turbulence, Wiley, NY, 397 pp.

- Pasquill, F., 1974: Atmospheric Diffusion. London, D. Van Nostrand Company Ltd. 297 pp.
- Passi, R. M., and C. Morel, 1987: Wind errors using the world-wide Loran network. J. Atmos. Oceanic Tech., 4, 690-700.
- Perry, S. G., A. B. Fraser, D. W. Thomson, and J. M. Norman, 1988: Indirect sensing of plant canopy structure with simple radiation measurements. Agric. and For. Meteor., 42, 255-278.
- Peterson, V. L., 1988: Wind Profiling. Tycho Technology, Inc. Boulder, CO.
- Pratt, R. W., 1985: Review of radiosonde humidity and temperature errors. J. Atmos. Oceanic Technol., 2, 404-407.
- Priestley, J. T., and R. J. Hill, 1985: Measuring high-frequency humidity, temperature, and radio refractive index in the surface layer. J. Atmos. and Oceanic Tech., 2, 233-251.
- Quality assurance handbook for air pollution measurement systems, Vol. IV Meteorological Measurements (August 1989), T. J. Lockhart, Ed. U.S. Environmental Protection Agency Atmospheric Research and Exposure Assessment Laboratory. Research Triangle Park, NC 27711.
- Randerson, D., Ed., 1984: Atmospheric Science and Power Production. DOE/TIC-27601 U.S. Dept. of Energy, Office of Scientific and Technical Information. DE84005177
- Richner, H., P. Ruppert, and B. Neininger, 1991: Performance characteristics of a miniaturized dew point mirror in air-borne and surface applications. Seventh Symp. on Meteor. Obs. and Instr., New Orleans, LA. AMS
- Schroeder, J. A., J. R. Jordan, and M. T. Decker, 1989: Design considerations for a network of thermodynamic profilers. J. Atmos. Oceanic Tech., 6, 840-845.
- Silverman, B., 1968: The effect of spatial averaging on spectrum estimation. J. Appl. Meteor., 7, 168-172.
- Singal, S. P., 1988: Acoustic-sounding studies of the atmospheric boundary layer. Scientific Report 30, New Zealand Meteorological Service, P.O. Box 722, Wellington, NZ.
- Snow, J. T., D. E. Lund, M. D. Conner, S. B. Harley, and C. B. Pedigo, 1989: On the dynamic response of a wind measuring system. J. Atmos. Oceanic Tech., 6, 140-146.

- Spizzichino, A., 1974: Discussion of the operating conditions of a Doppler sodar. J. Geophys. Research, 79, 5585-5591.
- Stevens, D. W., 1967: High-resolution measurement of air temperatures and temperature differences. J. Appl. Meteor., 6, 179-185.
- Strauch, R. G., B. L. Weber, A. S. Frisch, C. G. Little, D. A. Merritt, K. P. Moran, and D. C. Welsh, 1987: The precision and relative accuracy of profiler wind measurements. J. Atmos. Oceanic Tech., 4, 563-571.
- Strimaitis, D., G. Hoffnagle, and A. Bass, 1981: On-site meteorological instrumentation requirements to characterize diffusion from point sources. EPA-600/9-81-020 (April 1981). U.S. Environmental Protection Agency, Environmental Sciences Research Laboratory, Research Triangle Park, NC 27711.
- SurrIDGE, A. D., 1986: A review of radio acoustic sounding techniques. Council for Scientific and Industrial Research, CFI5108, Pretoria, South Africa.
- Susko, M., and W. W. Vaughan, 1968: Accuracy of wind data obtained by tracking a Jimsphere wind sensor simultaneously with two FPS-16 radars. NASA Technical Memorandum TMX-53752, Marshall Space Flight Center, AL.
- Tatarskii, V. I., 1961: Wave Propagation in a Turbulent Medium, Dover, NY (Translation by R. A. Silverman).
- Thompson, W. A., 1963: Precision of simultaneous measurement procedures. J. Amer. Statistical Assn., 58, 474-479.
- Touloukian, Y. S., and D. P. DeWitt: Thermophysical Properties of Matter, Volume 7, Thermal Radiative Properties, Metallic Elements and Alloys. IFI/Plenum, New York, 1970.
- Tsukamoto, O., 1986: Dynamic response of the fine wire psychrometer for direct measurement of water vapor flux. J. Atmos. Oceanic Tech., 3, 453-461.
- Uman, M. A., 1987: The Lightning Discharge, Academic Press, Orlando, FL, 377 pp.
- van de Kamp, D., 1988: Profiler training manual #1, Principles of Wind Profiler Operation. National Oceanic and Atmospheric Administration/Environmental Research Laboratory. Boulder, CO.
- Wade, C. G., 1987: A quality control program for surface meso-meteorological data. J. Atmos. Oceanic Tech., 4, 435-453.

- Wang, T-i, G. R. Ochs, D. A. Williams, N, Zeisser, and M. T. Nguyen, 1991: A long range scintillometer for atmospheric refractive turbulence. Scientific Technology, Inc. Final Report, Contract No. DOD-89-C-0031, U. S. Army Dugway Proving Ground, Dugway, UT 84022.
- Wiederhold, P. R., 1975: Humidity measurements. Instrumentation Technology, General Eastern Corporation, Watertown, MA.
- World Meteorological Organization (WMO), 1983: Guide to meteorological instrument and observing practices, 5th ed. WMO No. 8. TP3, Secretariat of the World Meteorological Organization, Geneva, Switz.
- Wyngaard, J. C., 1981: The effects of probe-induced flow distortion on atmospheric turbulence measurements. J. Appl. Meteor., 20, 784-794.